Chemical Evolution

Francesca Matteucci
Department of Astronomy
University of Trieste
and Osservatorio Astronomico di Trieste (INAF)
Via G.B. Tiepolo, 11, 34124 Trieste
Italy
(matteucci@ts.astro.it)

Contents

1 Chemical Evolution *page* 1

1.1 Lecture I: basic assumptions and equations of chemical evolution 1

1.1.1 The basic ingredients 1

1.1.2 The Star Formation Rate 2

1.1.3 The Initial Mass Function 3

1.1.4 The Infall Rate 4

1.1.5 The Outflow Rate 4

1.1.6 Stellar evolution and nucleosynthesis: the stellar yields 5

1.1.7 Type Ia SN Progenitors 6

1.1.8 Yields per Stellar Generation 7

1.1.9 Analytical models 8

1.1.10 Numerical Models 9

1.2 Lecture II: the Milky Way and other spirals 11

1.2.1 The Galactic formation timescales 11

1.2.2 The two-infall model 12

1.2.3 Common Conclusions from MW Models 18

1.2.4 Abundance Gradients from Emission Lines 19

1.2.5 Abundance Gradients in External Galaxies 21

1.2.6 How to model the Hubble Sequence 21

1.2.7 Type Ia SN rates in different galaxies 24

1.2.8 Time-delay model for different galaxies 25

1.3 Lecture III: interpretation of abundances in dwarf irregulars 27

1.3.1 Properties of Dwarf Irregular Galaxies 27

1.3.2 Galactic Winds 31

1.3.3 Results on DIG and BCG from purely chemical models 32
1.3.4 Results from Chemo-Dynamical models: IZw18 34
1.4 Lecture IV: Elliptical galaxies-Quasars- ICM Enrichment 38
1.4.1 Ellipticals 38
1.4.2 Chemical Properties 38
1.4.3 Scenarios for galaxy formation 39
1.4.4 Ellipticals-Quasars connection 41
1.4.5 The chemical evolution of QSOs 41
1.4.6 The chemical enrichment of the ICM 43
1.4.7 Conclusions on the enrichment of the ICM 46
References 48

1

Chemical Evolution

1.1 Lecture I: basic assumptions and equations of chemical evolution

To build galaxy chemical evolution models one needs to elucidate a number of hypotheses and make assumptions on the basic ingredients.

1.1.1 The basic ingredients

- INITIAL CONDITIONS: whether the mass of gas out of which stars will form is all present initially or it will be accreted later on. The chemical composition of the initial gas (primordial or already enriched by a pregalactic stellar generation).
- THE BIRTHRATE FUNCTION:

$$B(M,t) = \psi(t)\varphi(M) \tag{1.1}$$

where:

$$\psi(t) = SFR \tag{1.2}$$

is the star formation rate (SFR) and:

$$\varphi(M) = IMF \tag{1.3}$$

is the initial mass function (IMF).

- STELLAR EVOLUTION AND NUCLEOSYNTHESIS: stellar yields, yields per stellar generation
- SUPPLEMENTARY PARAMETERS : infall, outflow, radial flows.

1.1.2 The Star Formation Rate

Here we will summarize the most common parametrizations for the SFR in galaxies, as adopted by chemical evolution models:

- Constant in space and time and equal to the estimated present time SFR. For example, for the local disk, the present time SFR is SFR=2-5$M_{\odot}pc^{-2}Gyr^{-1}$ (Boissier& Prantzos, 1999).
- Exponentially decreasing:

$$SFR = \nu e^{-t/\tau_*} \tag{1.4}$$

  with $\tau_* = 5 - 15$ Gyr (Tosi, 1988). The quantity $\nu$is a parameter that we call efficiency of SF since it represents the SFR per unit mass of gas and is expressed in Gyr^{-1}.
- The most used SFR is the Schmidt (1959) law, which assumes a dependence on the gas density, in particular:

$$SFR = \nu\sigma_{gas}^{k} \tag{1.5}$$

  where $k = 1.4 \pm 0.15$, as suggested by a study of Kennicutt (1998) of local star forming galaxies.
- Some variations of the Schmidt law with a dependence also on the total mass have been suggested for example by Dopita & Ryder (1994). This formulation takes into account the feedback mechanism acting between supernovae (SNe) and stellar winds injecting energy into the interstellar medium (ISM) and the galactic potential well. In other words, the SF process is regulated by the fact that in a region of recent star formation the gas is too hot to form stars and it is easily removed from that region. Before new stars could form the gas needs to cool and collapse back into the star forming region and this process depends on the potential well and therefore on the total mass density:

$$SFR = \nu\sigma_{tot}^{k_1}\sigma_{gas}^{k_2} \tag{1.6}$$

  with $k_1 = 0.5$ and $k_2 = 1.5$.
- Kennicutt (1998) also suggested, as an alternative to the Schmidt law to fit the data, the following relation:

$$SFR = 0.017\Omega_{gas}\sigma_{gas} \propto R^{-1}\sigma_{gas} \tag{1.7}$$

  with Ω_{gas} being the angular rotation speed of gas.

- Finally a SFR induced by spiral density waves was suggested by Wyse & Silk (1989):

$$SFR = \nu V(R) R^{-1} \sigma_{gas}^{1.5} \tag{1.8}$$

with R being the galactocentric distance and $V(R)$ the gas rotation velocity.

1.1.3 The Initial Mass Function

The IMF is a probability function describing the distribution of stars as a function of mass. The present day mass function is derived for the stars in the solar vicinity by counting the Main Sequence stars as a function of magnitude and then applying the mass-luminosty relation, holding for Main Sequence stars, to derive the distribution of stars as a function of mass. In order to derive the IMF one has then to make assumptions on the past history of SF.

The derived IMF is normally approximated by a power law:

$$\varphi(M)dM = aM^{-(1+x)}dM \tag{1.9}$$

where $\varphi(M)$ is the number of stars with masses in the interval M, M+dM.

Salpeter (1955) proposed a one-slope IMF ($x = 1.35$) valid for stars with $M > 10M_{\odot}$. Multi-slope (x_1, x_2, ..) IMFs have been suggested later on always for the solar vicinity (Scalo 1986,1998; Kroupa et al. 1993; Chabrier 2003). The IMF is generally normalized as:

$$a \int_{0.1}^{100} M\varphi(M)dM = 1 \tag{1.10}$$

where a is the normalization constant and the assumed interval of integration is $0.1 - 100M_{\odot}$.

The IMF is generally considered constant in space and time with some exceptions such as the IMF suggested by Larson (1998) with:

$$x = 1.35(1 + m/m_1)^{-1} \tag{1.11}$$

where m_1 is variable typical mass and is associated to the Jeans mass. This IMF predicts then that m_1 is a decreasing function of time.

1.1.4 The Infall Rate

For the rate of gas accretion there are in the literature several parametrizations:

- The infall rate is constant in space and time and equal to the present time infall rate as measured in the Galaxy ($\sim 1.0 M_{\odot} yr^{-1}$).
- The infall rate is variable in space and time, and the most common assumption is an exponential law (Chiosi 1980; Lacey & Fall 1985):

$$IR = A(R)e^{-t/\tau(R)} \tag{1.12}$$

  with $\tau(R)$ constant or varying with the galactocentric distance. The parameter $A(R)$ is derived by fitting the present day total surface mass density, $\sigma_{tot}(t_G)$, at any specific galactocentric radius R.
- For the formation of the Milky Way two episodes of infall have been suggested (Chiappini et al. 1997), where during the first infall episode the stellar halo forms whereas during the second infall episode the disk forms. This particular infall law gives a good representation of the formation of the Milky Way. The proposed two-infall law is:

$$IR = A(R)e^{-t/\tau_H(R)} + B(R)e^{-(t-t_{max})/\tau_D(R)} \tag{1.13}$$

  where $\tau_H(R)$ is the timescale for the formation of the halo which can be costant or vary with galactocentric distance. The quantity $\tau_D(R)$ is the timescale for the formation of the disk and is a function of the galactocentric distance; in most of the models it is assumed to increase with R (e.g. Matteucci & François, 1989).
- More recently, Prantzos (2003) suggested a gaussian law with a peak at 0.1 Gyr and a FWHM of 0.04 Gyr for the formation of the stellar halo.

1.1.5 The Outflow Rate

The so-called galactic winds occur when the thermal energy of the gas in galaxies exceeds its potential energy. Generally, gas outflows are called winds when the gas is lost forever from the galaxy. Only detailed dynamical simulations can suggest whether there is a wind or just an outflow of gas which will soon or later fall back again into the galaxy. In chemical evolution models galactic winds can be sudden or continuous. If they are sudden, the mass is assumed to be lost in a very short interval of

time and the galaxy is devoided from all the gas; if they are continuous, one has to assume the rate of gas loss. Generally, in chemical evolution models (Bradamante et al. 1998) and also in cosmological simulations (Springel & Hernquist, 2003) it is assumed that the rate of gas loss is several times the SFR:

$$W = -\lambda SFR \tag{1.14}$$

where λ is a free parameter with the meaning of wind efficiency. This particular formulation for the galactic wind rate is confirmed by observational findings (see Martin, 1999).

1.1.6 Stellar evolution and nucleosynthesis: the stellar yields

Here we summarize the various contribution to the element production by stars of all masses.

- Brown Dwarfs ($M < M_L$, $M_L = 0.08 - 0.09 M_\odot$) are objects which never ignite H and their lifetimes are larger than the age of the Universe. They are contributing to lock up mass.
- Low mass stars ($0.5 \leq M/M_\odot \leq M_{HeF}$) (1.85-2.2$M_\odot$) ignite He explosively but without destroying themselves and then become C-O white dwarfs (WD). If $M < 0.5 M_\odot$ they become He WDs. Their lifetimes range from several 10^9 years up to several Hubble times!
- Intermediate mass stars ($M_{HeF} \leq M/M_\odot \leq M_{up}$) ignite He quiescently. The mass M_{up} is the limiting mass for the formation of a C-O degenerate core and is in the range 5-9$M_\odot$, depending on stellar evolution calculations. Lifetimes are from several 10^7 to 10^9 years. They die as C-O WDs if not in binary systems. If in binary systems they can give rise to cataclysmic variables such as novae and Type Ia SNe.
- Massive stars ($M > M_{up}$). We distinguish here several cases:

  -$M_{up} \leq M/M_\odot \leq 10 - 12$. Stars with Main Sequence masses in this range end up as electron-capture SNe leaving neutron stars as remnants. These SNe will appear as Type II SNe which show H in their spectra.

  -$10 - 12 \leq M/M_\odot \leq M_{WR}$, (with $M_{WR} \sim 20 - 40 M_\odot$ being the limiting mass for the formation of a Wolf-Rayet (WR) star). Stars in this mass range end their life as core-collapse SNe (Type II) leaving a neutron star or a black hole as remnants.

  -$M_{WR} \leq M/M_\odot \leq 100$. Stars in this mass range are probably

exploding as Type Ib/c SNe which do not show H in their spectra. Their lifetimes are of the order of $\sim 10^6$ years.

- Very Massive Stars ($M > 100 M_\odot$), they should explode by means of instability due to "pair creation" and they are called *pair-creation* SNe. In fact, at $T \sim 2 \cdot 10^9$ K a large portion of the gravitational energy goes into creation of pairs (e^+, e^-), the star becomes unstable and explodes. They leave no remnants and their lifetimes are $< 10^6$ years. Probably these very massive stars formed only when the metal content was almost zero (Population III stars, Schneider et al. 2004).

All the elements with mass number A from 12 to 60 have been formed in stars during the quiescent burnings. Stars transform H into He and then He into heaviers until the Fe-peak elements, where the binding energy per nucleon reaches a maximum and the nuclear fusion reactions stop.

H is transformed into He through the proton-proton chain or the CNO-cycle, then ^4He is transformed into ^{12}C through the triple- α reaction.

Elements heavier than ^{12}C are then produced by synthesis of α-particles. They are called α-elements (O, Ne, Mg, Si and others).

The last main burning in stars is the ^{28}Si -burning which produces ^{56}Ni which then decays into ^{56}Co and ^{56}Fe. Si-burning can be quiescent or explosive (depending on the temperature).

Explosive nucleosynthesis occurring during SN explosions mainly produces Fe-peak elements. Elements originating from s- and r-processes (with A> 60 up to Th and U) are formed by means of slow or rapid (relative to the β- decay) neutron capture by Fe seed nuclei; s-processing occurs during quiescent He-burning whereas r-processing occurs during SN explosions.

1.1.7 Type Ia SN Progenitors

The Type Ia SNe, which do not show H in their spectra, are believed to originate from WDs in binary systems and to be the major producers of Fe in the Universe. The model proposed are basically two:

- **Single Degenerate Scenario (SDS)**, with a WD plus a Main Sequence or Red Giant star, as originally suggested by Whelan and Iben (1973). The explosion (C-deflagration) occurs when the C-O WD reaches the Chandrasekhar mass, $M_{Ch} =\sim 1.44 M_\odot$, after accreting material from thecompanion. In this model the clock to the explosion is given by the lifetime of the companion of the WD (namely the less

massive star in the system). It is interesting to define the minimum timescale for the explosion which is given by the lifetime of a $8M_{\odot}$ star, namely $t_{SNIa_{min}}$=0.03 Gyr (Greggio and Renzini 1983). Recent observations in radio-galaxies by Mannucci et al. (2005;2006) seem to confirm the existence of such prompt Type Ia SNe.

- **Double Degenerate Scenario (DDS)**, where the merging of two C-O WDs of mass $\sim 0.7M_{\odot}$, due to loss of angular momentum as a consequence of gravitational wave radiation, produces C-deflagration (Iben and Tutukov 1984). In this case the clock to the explosion is given by the lifetime of the secondary star, as above, plus the gravitational time delay, namely the time necessary for the two WDs to merge. The minimum time for the explosion is $t_{SNIa_{min}} = 0.03 + \Delta t_{grav}$=0.04 Gyr (see Tornambè 1989).

Some variations of the above scenarios have been proposed such as the model by Hachisu et al. (1996; 1999), which is based on the single degenerate scenario where a wind from the WD is considered. Such a wind stabilizes the accretion from the companion and introduces a metallicity effect. In particular, the wind, necessary to this model, occurs only if the systems have metallicity ([Fe/H]< -1.0). This implies that the minimum time for the explosion is larger than in the previous cases. In particular, $t_{SNIa_{min}} = 0.33$ Gyr, which is the lifetime of the more massive secondary considered ($2.3M_{\odot}$) plus the metallicity delay which depends on the assumed chemical evolution model.

1.1.8 Yields per Stellar Generation

Under the assumption of Instantaneous Recycling Approximation (IRA) which states that all stars more massive than $1M_{\odot}$ die immediately, whereas all stars with masses lower than $1M_{\odot}$ live forever, one can define the yield per stellar generation (Tinsley, 1980);

$$y_i = \frac{1}{1-R}\int_1^{\infty} m p_{im} \varphi(m) dm \tag{1.15}$$

where p_{im} is the stellar yield of the element i, namely the newly formed and ejected element i by a star of mass m.

The quantity R is the so-called Returned Fraction:

$$R = \int_1^{\infty} (m - M_{rem}) \varphi(m) dm \tag{1.16}$$

and is the total mass of gas restored into the ISM by an entire stellar generation.

1.1.9 Analytical models

The *Simple Model* for the chemical evolution of the solar neighbourhood is the simplest approach to model chemical evolution. The solar neighbourhood is assumed to be a cylinder of 1 Kpc radius centered around the Sun.

The basic assumptions of the Simple Model are:

- the system is one-zone and closed, no inflows or outflows with the total mass present since the beginning,
- the initial gas is primordial (no metals),
- instantaneous recycling approximation holds,
- the IMF, $\varphi(m)$, is assumed to be constant in time,
- the gas is well mixed at any time (IMA)

The Simple Model fails in describing the evolution of the Milky Way (G-dwarf metallicity distribution, elements produced on long timescales and abundance ratios) and the reason is that at least two of the above assumptions are manifestly wrong, epecially if one intends to model the evolution of the abundance of elements produced on long timescales, such as Fe. In particular the assumptions of the closed boxiness and the IRA.

However, it is interesting to know the solution of the Simple Model and its implications. Be X_i the abundance by mass of an element i.

If $X_i << 1$, which is generally true for metals, we obtain the solution of the Simple Model. This solution is obtained analytically by ignoring the stellar lifetimes:

$$X_i = y_i ln(\frac{1}{G}) \tag{1.17}$$

where $\mu = M_{gas}/M_{tot}$ and y_i is the yield per stellar generation, as defined above, otherwise called *effective yield*. In particular, the effective yield is defined as:

$$y_{i_{eff}} = \frac{X_i}{ln(1/G)} \tag{1.18}$$

namely the yield that the system would have if behaving as the simple closed-box model. This means that if $y_{i_{eff}} > y_i$, then the actual system has attained a higher abundance for the element i at a given gas fraction G. Generally, in the IRA, we can assume:

$$\frac{X_i}{X_j} = \frac{y_i}{y_j} \tag{1.19}$$

which means that the ratio of two element abundances are always equal to the ratio of their yields. This is no more true when IRA is relaxed. In fact, relaxing IRA is necessary to study in detail the evolution of the abundances of single elements.

One can obtain analytical solutions also in presence of infall and/or outflow but the necessary condition is to assume IRA. Matteucci & Chiosi (1983) found solutions for models with outflow and infall and Matteucci (2001) found it for a model with infall and outflow acting at the same time. The main assumption in the model with outflow but no infall is that the outflow rate is:

$$W(t) = \lambda(1 - R)\psi(t) \tag{1.20}$$

where $\lambda \geq 0$ is the wind parameter.

The solution of this model is:

$$X_i = \frac{y_i}{(1+\lambda)} ln[(1+\lambda)G^{-1} - \lambda] \tag{1.21}$$

for $\lambda = 0$ the equation becomes the one of the Simple Model (1.17).

The solution of the equation of metals for a model without wind but with a primordial infalling material ($X_{A_i} = 0$) at a rate:

$$A(t) = \Lambda(1 - R)\psi(t) \tag{1.22}$$

and $\Lambda \neq 1$ is :

$$X_i = \frac{y_i}{\Lambda}[1 - (\Lambda - (\Lambda - 1)G^{-1})^{-\Lambda/(1-\Lambda)}] \tag{1.23}$$

For $\Lambda = 1$ one obtains the well known case of *extreme infall* studied by Larson (1972) whose solution is:

$$X_i = y_i[1 - e^{-(G^{-1}-1)}] \tag{1.24}$$

This extreme infall solution shows that when $G \to 0$ then $X_i \to y_i$.

1.1.10 Numerical Models

Numerical models relax IRA and close boxiness but generally retain the constancy of $\varphi(m)$ and the IMA.

If G_i is the mass fraction of gas in the form of an element i, we can write:

$$\begin{aligned}
&\dot{G}_i(t) = -\psi(t)X_i(t) \\
&+\int_{M_L}^{M_{Bm}} \psi(t-\tau_m)Q_{mi}(t-\tau_m)\varphi(m)dm \\
&+A\int_{M_{Bm}}^{M_{BM}} \phi(m) \\
&\cdot[\int_{\mu_{min}}^{0.5} f(\gamma)\psi(t-\tau_{m2})Q_{mi}(t-\tau_{m2})d\gamma]dm \\
&+B\int_{M_{Bm}}^{M_{BM}} \psi(t-\tau_m)Q_{mi}(t-\tau_m)\varphi(m)dm \\
&+\int_{M_{BM}}^{M_U} \psi(t-\tau_m)Q_{mi}(t-\tau_m)\varphi(m)dm \\
&+X_{A_i}A(t) - X_i(t)W(t)
\end{aligned} \tag{1.25}$$

where B=1-A, A=0.05-0.09. The meaning of the A parameter is the fraction in the IMF of binary systems with those specific features required to give rise to Type Ia SNe, whereas B is the fraction of all the single stars and binary systems in the same mass range of definition of the progenitors of Type Ia SNe. The values of A indicated above are correct for the evolution of the solar vicinity where an IMF of Scalo (1986, 1989) or Kroupa et al.(1993) is adopted. If one adopts a flatter IMF such as the Salpeter (1955) one then A is different. In the above equations the contribution of Type Ia SNe is contained in the third term on the right hand side. The integral is made over a range of masses going from 3 to 16 $M_\odot$ which represents the total masses of binary systems able to produce Type Ia SNe in the framework of the SDS. There is also an integration over the mass distribution of binary systems; in particular, one considers the function $f(\gamma)$ where $\gamma = \frac{M_2}{M_1+M_2}$, with M_1 and M_2 being the primary and secondary mass of the binary system, respectively (for more details see Matteucci & Greggio 1986 and Matteucci 2001).The functions A(t) and W(t) are the infall and wind rate, respectively. Finally, the quantity Q_{mi} represents the stellar yields (both processed and unprocessed material).

1.2 Lecture II: the Milky Way and other spirals

The Milky Way galaxy has four main stellar populations: 1) the halo stars with low metallicities (the most common metallicity indicator in stars is [Fe/H]= $log(Fe/H)_* - log(Fe/H)_\odot$) and eccentric orbits, 2) the bulge population with a large range of metallicities and is dominated by random motions, 3) the thin disk stars with an average metallicity $< [Fe/H] >$=-0.5 dex and circular orbits, and finally 4) the thick stars which possess chemical and kinematical properties intermediate between those of the halo and those of the thin disk. The halo stars have average metallicities of $< [Fe/H] >$=-1.5 dex and a maximum metallicity of ~ -1.0 dex although stars with [Fe/H] as high as -0.6 dex and halo kinematics are observed. The average metallicity of thin disk stars is ~ -0.6 dex, whereas the one of Bulge stars is ~ -0.2 dex.

1.2.1 The Galactic formation timescales

The kinematical and chemical properties of the different Galactic stellar populations can be interpreted in terms of the Galaxy formation mechanism. Eggen et al. (1962) in a cornerstone paper suggested a rapid collapse for the formation of the Galaxy lasting $\sim 3 \cdot 10^8$ years. This suggestion was based on a kinematical and chemical study of solar neighbourhood stars. Later on, Searle & Zinn (1979) proposed a central collapse like the one proposed by Eggen et al. but also that the outer halo formed by merging of large fragments taking place over a considerable timescale > 1 Gyr. More recently, Berman & Suchov (1991) proposed the so-called hot Galaxy picture, with an initial strong burst of SF which inhibited further SF for few Gyr while a strong Galactic wind was created.

From an historical point of view, the modelization of the Galactic chemical evolution has passed through different phases that I summarize in the following.

- SERIAL FORMATION

  The Galaxy is modeled by means of one accretion episode lasting for the entire Galactic lifetime, where halo, thick and thin disk form in sequence as a continuous process. The obvious limit of this approach is that it does not allow us to predict the observed overlapping in metallicity between halo and thick disk stars and between thick and thin disk stars, but it gives a fair representation of our Galaxy (e.g. Matteucci & François 1989).

- PARALLEL FORMATION

  In this formulation, the various Galactic components start at the same time and from the same gas but evolve at different rates (e.g. Pardi et al. 1995). It predicts overlapping of stars belonging to the different components but implies that the thick disk formed out of gas shed by the halo and that the thin disk formed out of gas shed by the thick disk, and this is at variance with the distribution of the stellar angular momentum per unit mass (Wyse & Gilmore 1992), which indicates that the disk did not form out of gas shed by the halo.
- TWO-INFALL FORMATION

  In this scenario, halo and disk formed out of two separate infall episodes (overlapping in metallicity is also predicted) (e.g. Chiappini et al. 1997; Chang et al. 1999). The first infall episode lasted no more than 1-2 Gyr whereas the second, where the thin disk formed, lasted much longer with a timescale for the formation of the solar vicinity of 6-8 Gyr (Chiappini et al. 1997; Boissier& Prantzos 1999).
- STOCHASTIC APPROACH

  Here the hypothesis is that in the early halo phases ([Fe/H] < -3.0 dex), mixing was not efficient and, as a consequence, one should observe in low metallicity halo stars the effects of pollution from single SNe (e.g. Tsujimoto et al. 1999; Argast et al. 2000; Oey 2000). These models predict a large spread for [Fe/H] < -3.0dex which is not observed, as shown by recent data with metallicities down to -4.0 dex (Cayrel et al. 2004; see later).

1.2.2 The two-infall model

The adopted SFR (see Figure 2.1) is eq.(1.6) with different SF efficiencies for the halo and disk, in particular $\nu_H = 2.0 Gyr^{-1}$, $\nu_D = 1.0 Gyr^{-1}$, respectively. A threshold density ($\sigma_{th} = 7 M_{\odot} pc^{-2}$) for the SFR is also assumed in agreement with results from Kennicutt (1989; 1998).

In Figure 2.2 we show the predicted SN (II and Ia) rates by the two-infall model. Note that the Type Ia SN rate is calculated according to the SDS (Greggio & Renzini, 1983; Matteucci & Recchi, 2001). There is a delay between the Type II SN rate and the Type Ia SN rate, and while the Type II SN rate strictly follows the SFR, the Type Ia SN rate is smoothly increasing.

François et al. (2004) compared the predictions of the two-infall model for the abundance ratios versus metallicity relations ([X/Fe] vs. [Fe/H]), with the very recent and very accurate data of the project "First Stars"

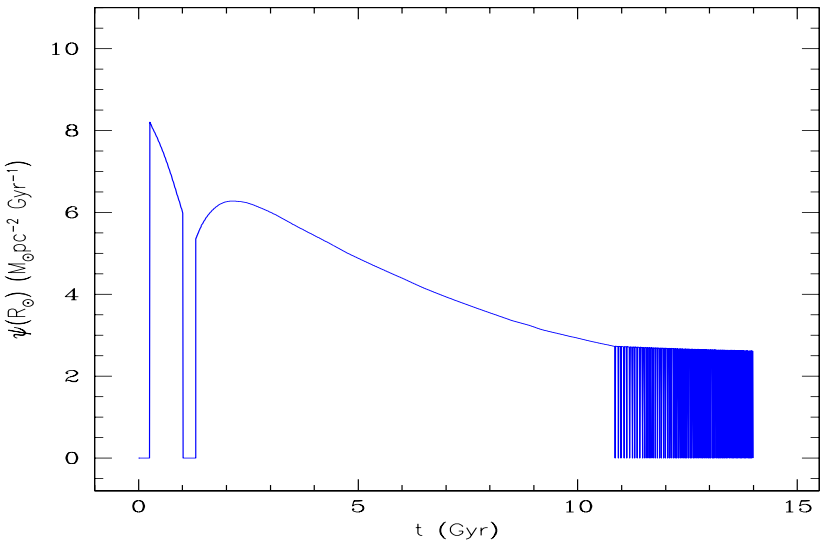

Fig. 1.1. The predicted SFR in the solar vicinity with the two-infall model. Figure from Chiappini et al. (1997). The oscillating behaviour at late times is due to the assumed threshold density for SF. The threshold gas density is also responsible for the gap in the SFR seen at around 1 Gyr.

by Cayrel et al. (2004). They adopted yields from the literature both for Type II and Type Ia SNe and noticed that while for some elements (O, Fe, Si, Ca) the yields of Woosley & Weaver (1995) (hereafter WW95) reproduce the data fairly well, for the Fe-peak elements and heaviers none of the available yields give a good agreement. Therefore, they varied empirically the yields of these elements in order to best fit the data. In Figures 2.3 and 2.4 we show the predictions for α-elements (O, Mg, Si, Ca, Ti, K) plus some Fe-peak elements and Zn.

In Figure 2.4 we show also the ratios between the yields derived empirically by François et al. (2004) in order to obtain the excellent fits shown in the figures, and those of WW95 for massive stars. For some elements it was necessary to change also the yields from Type Ia SNe relative to the reference ones which are those of Iwamoto et al. (1999) (hereafter I99).

In Figure 2.5 we show the predictions of chemical evolution models for ^{12}C and ^{14}N compared with abundance data. The behaviour of C shows a roughly constant [C/Fe] as a function of [Fe/H], although C seems to

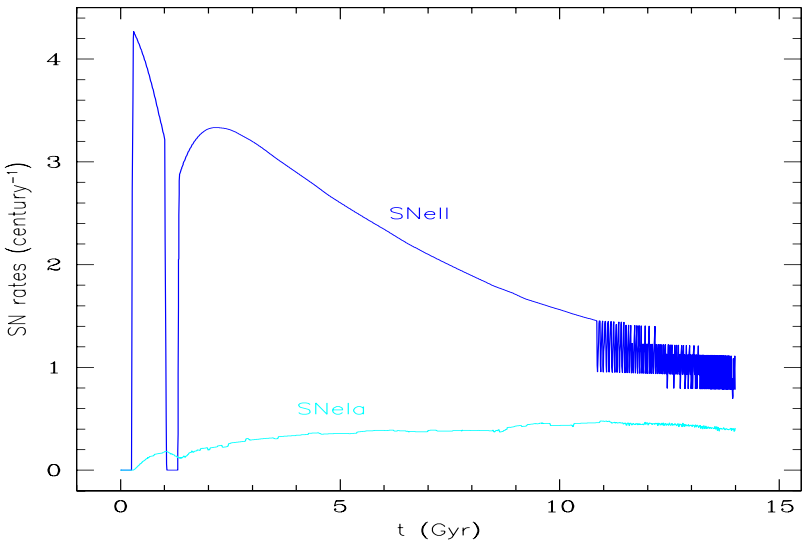

Fig. 1.2. The predicted Type II and Ia SN rate in the solar vicinity with the two-infall model. Figure from Chiappini et al. (1997)

slightly increase at very low metallicities, indicating that the bulk of these two elements comes from stars with the same lifetimes. The data in these figures, especially those for N are old and do not contain very metal poor stars. Newer data containing stars with [Fe/H] down to $\sim$ -4.0 dex (Spite et al. 2005; Israelian et al. 2004) indicate that the [N/Fe] ratio continues to be high also at low metallicities, indicating a primary origin for N produced in massive stars. We recall here that we define *primary* a chemical elements which is produced in the stars starting from the H and He, whereas we define *secondary* a chemical element which is formed from heavy elements already present in the star at its birth and not produced in situ. The model predictions shown in Figure 2.5 for C and N assume that the bulk of these elements is produced by low and intermediate mass stars (yields from van den Hoeck and Groenewegen, 1997) and that N is produced as a partly secondary and partly primary element. The N production from massive stars has only a secondary origin (yields from WW95). In Figure 2.5 we show also a model prediction where N is considered as a primary element in massive stars with the yields artificially increased. Recently, Chiappini et al.

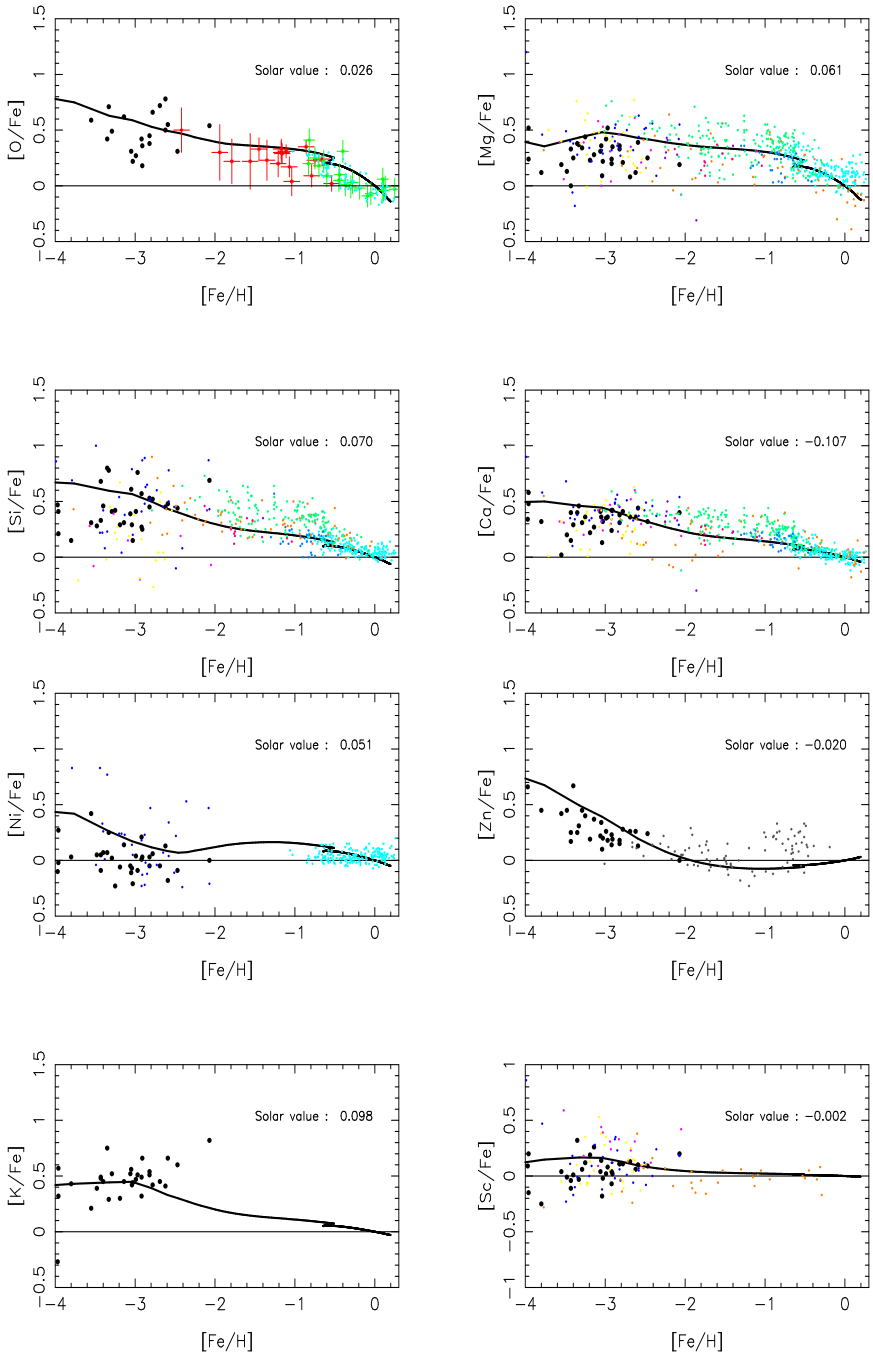

Fig. 1.3. Predicted and observed [X/Fe] vs. [Fe/H] for several α- and Fe-peak-elements plus Zn compared with a compilation of data. In particular the black dots are the recent high resolution data from Cayrel et al. (2004). For the other data see references in François et al. (2004). The solar value indicated in the upper right part of each figure represents the predicted solar value for the ratio [X/Fe]. The assumed solar abundances are those of Grevesse & Sauval (1998) except that for oxygen for which we take the value of Holweger (2001).

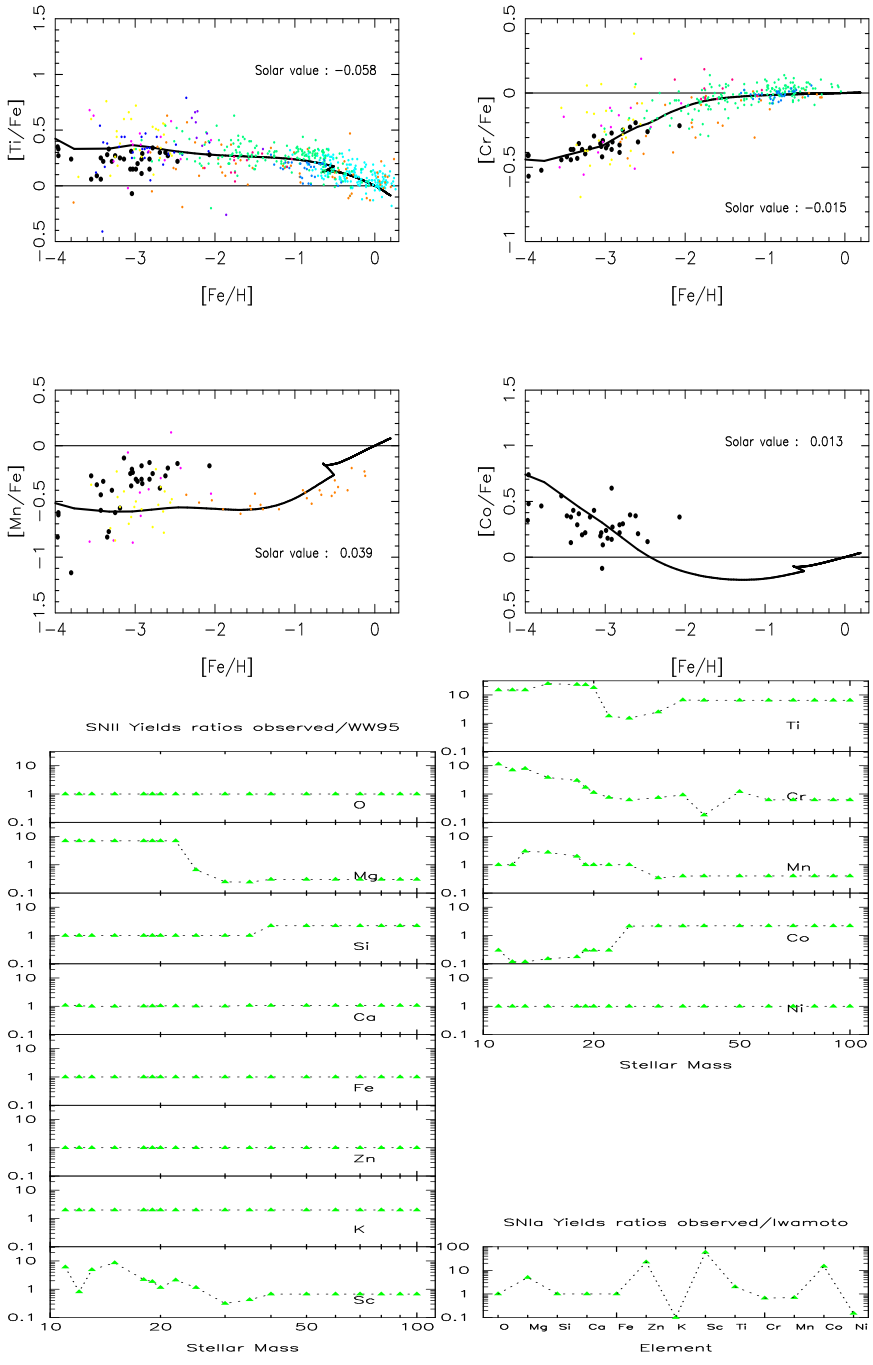

Fig. 1.4. Upper panel: predicted and observed [X/Fe] vs. [Fe/H] for several elements as in Figure 2.3. In the bottom part of this Figure are shown the ratios between the empirical yields and the yields by WW95 for massive stars. Such empirical yields have been suggested by François et al. (2004) in order to fit at best all the [X/Fe] vs. [Fe/H] relations. In the small panel at the bottom right side are shown also the ratios between the empirical yields for Type Ia SNe and the yields by I99.

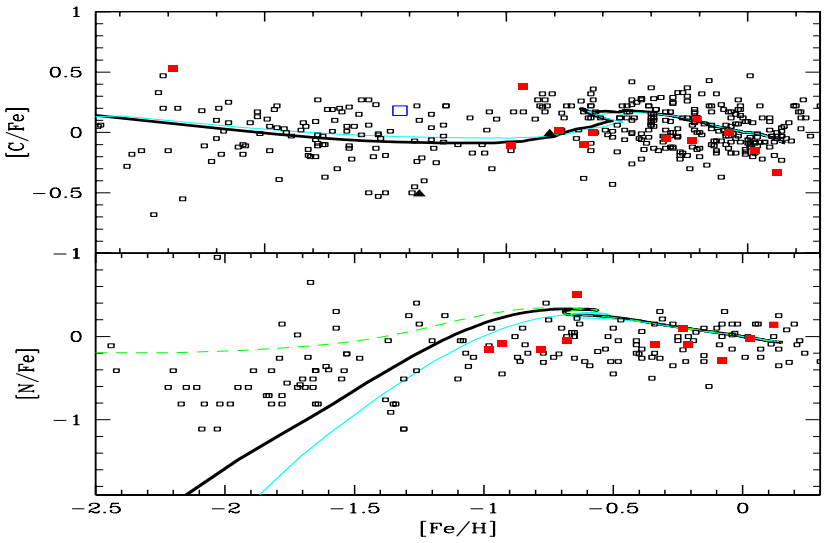

Fig. 1.5. Upper panel: predicted and observed [C/Fe] vs. [Fe/H]. Models from Chiappini et al. (2003a). Lower panel, predicted and observed [N/Fe] vs. [Fe/H]. For references to the data see original paper.The thin and thick continuous lines in both panels represent models with standard nucleosynthesis, as described in the text, whereas the dashed line represents the predictions of a model where N in massive stars has been considered as a primary element with "ad hoc" stellar yields.

(2006) have shown that primary N produced by very metal poor fastly rotating massive stars can well reproduce the observations.

In summary, the comparison between model predictions and abundance data indicate the following scenario for the formation of heavy elements:

- ^{12}C and ^{14}N are mainly produced in low and intermediate mass stars ($0.8 \leq M/M_{\odot} \leq 8$). The amounts of primary and secondary N is still uncertain and also the fraction of C produced in massive stars. Primary N from massive stars seems to be required to reproduce the N abundance in low metallicity halo stars.
- α-elements originate in massive stars: the nucleosynthesis of O is rather well understood (there is agreement between different authors), the yields from WW95 as functions of metallicity produce an excellent agreement with the observations for this particular element.

- Magnesium is generally underproduced by nucleosynthesis models. Taking the yields of WW95 as a reference, the Mg yields should be increased in stars with masses $M \leq 20M_{\odot}$ and decreased in stars with $M > 20M_{\odot}$ to fit the data. Silicon should be slightly increased in stars with masses $M > 40M_{\odot}$.
- Fe originates mostly in Type Ia SNe. The Fe yields in massive stars are still uncertain, WW95 metallicity dependent yields overestimate Fe in stars $< 30M_{\odot}$. For this element, it is better to adopt the yields of WW95 for solar metallicity.
- Fe-peak elements: the yields of Cr, Mn should be increased in stars of 10-20 $M_{\odot}$ relative to the yields of WW95, whereas the yield of Co should be increased in Type Ia SNe, relative to the yields of I99, and decreased in stars in the range 10-20$M_{\odot}$, relative to the yields of WW95. Finally, the yield of Ni should be decreased in Type Ia SNe.
- The yields of Cu and Zn from Type Ia SNe should be larger, relative to the standard yields, as already suggested by Matteucci et al. (1993).

1.2.3 Common Conclusions from MW Models

Most of the chemical evolution models for the Milky Way existing in the literature conclude that:

- The G-dwarf metallicity distribution can be reproduced only by assuming a slow formation of the local disk by infall. In particular, the time-scale for the formation of the local disk should be in the range $\tau_d \sim 6 - 8$ Gyr (Chiappini et al. 1997; Boissier and Prantzos 1999; Chang et al. 1999; Chiappini et al. 2001; Alibès et al. 2001).
- The relative abundance ratios [X/Fe] vs. [Fe/H], interpreted as time-delay between Type Ia and II SNe, suggest a timescale for the halo-thick disk formation of $\tau_h \sim 1.5$-2.0 Gyr (Matteucci and Greggio 1986; Matteucci and François, 1989; Chiappini et al. 1997). The external halo and thick disk probably formed more slowly or have been accreted (Chiappini et al. 2001).
- To fit abundance gradients, SFR and gas distribution along the Galactic thin disk we must assume that the disk formed *inside-out* (Matteucci & François, 1989; Chiappini et al. 2001; Boissier & Prantzos 1999; Alibés et al. 2001). Radial flows can help in forming the gradients (Portinari & Chiosi 2000) but they are probably not the main cause for them. A variable IMF along the Disk can in principle explain abundance gradients but it creates unrealistic situations: in fact,

in order to reproduce the negative gradients one should assume that in the external and less metal rich parts of the Disk low mass stars form preferentially (see Chiappini et al. 2000 for a discussion on this point).

- The SFR is a strongly varying function of the galactocentric distance (Matteucci & François 1989; Chiappini et al, 1997,2001; Goswami & Prantzos 2000; Alibés et al. 2001).

1.2.4 Abundance Gradients from Emission Lines

There are two types of abundance determinations in HII regions: one is based on recombination lines which should have a weak temperature dependence of the nebula (He, C, N, O), the other is based on collisionally excited lines where a strong dependence is intrinsic to the method (C, N, O, Ne, Si, S, Cl, Ar, Fe and Ni). This second method has predominated until now. A direct determination of the abundance gradients from HII regions in the Galaxy from optical lines is difficult because of extinction, so usually the abundances for distances larger than 3 Kpc from the Sun are obtained from radio and infrared emission lines.

Abundance gradients can also be derived from optical emission lines in Planetary Nebulae (PNe). However, the abundances of He, C and N in PNe are giving only information on the internal nucleosynthesis of the star. So, to derive gradients one should look at the abundances of O, S and Ne, unaffected by stellar processes. In Figure 2.6 we show theoretical predictions of abundance gradients along the disk of the Milky Way compared with data from HII regions and B stars. The adopted model is from Chiappini et al. (2001; 2003a) and is based on an inside-out formation of the thin disk with the inner regions forming faster than the outer ones, in particular $\tau(R) = 0.875R - 0.75$ Gyr. Note that to obtain a better fit for ^{12}C, the yields of this element have been increased artificially relative to those of WW95.

As already said, most of the models agree on the inside-out scenario for the Disk formation, however not all models agree on the evolution of the gradients with time. In fact, some models predict a flattening with time (Boissier and Prantzos 1998; Alibès et al. 2001), whereas others such as that of Chiappini et al. (2001) predict a steepening. The reason for the steepening is that in the model of Chiappini et al. is included a threshold density for SF,, which induces the SF to stop when the density decreases below the threshold. This effect is particularly strong in the external regions of the Disk, thus contributing to a slower evolution and

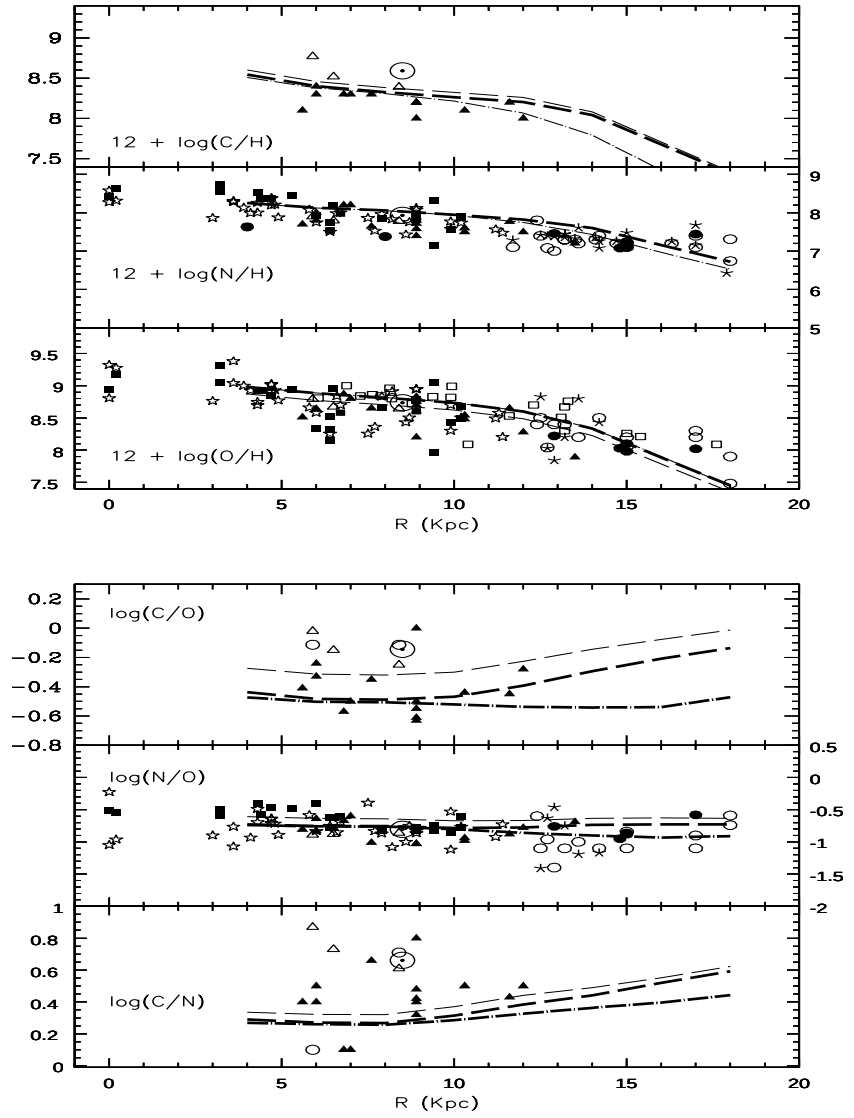

Fig. 1.6. Upper panel: abundance gradients along the Disk of the MW. The lines are the models from Chiappini et al. (2003a): these models differ by the nucleosynthesis prescriptions. In particular, the dash-dotted line represents a model with van den Hoeck & Groenewegen (1997, hereafter HG97) yields for low-intermediate mass stars with η (mass loss parameter) constant and Thielemann et al.'s (1996) yields for massive stars, the long- dashed thick line has HG97 yields with variable η and Thielemann et al. yields, the long-dashed thin line has HG97 yields with variable η but WW95 yields for massive stars. It is interesting to note that in all of these models the yields of ^{12}C in stars $> 40 M_{\odot}$ have been artificially increased by a factor of 3 relative to the yields of WW95. Lower panel: the temporal behaviour of abundance gradients along the Disk as predicted by the best model of Chiappini et al. (2001). The upper lines in each panel represent the present time gradient, whereas the lower ones represent the gradient a few Gyr ago. It is clear that the gradients tend to stepeen in time, a still controversial result.

therefore to a steepening of the gradients with time, as shown in Figure 2.6, bottom panel.

1.2.5 Abundance Gradients in External Galaxies

Abundance gradients expressed in dex/Kpc are found to be steeper in smaller disks but the correlation disappears if they are expressed in dex/R_d, which means that there is a universal slope per unit scale length (ref). The gradients are generally flatter in galaxies with central bars (ref). The SFR is measured mainly from H_α emission (Kennicutt, 1998) and show a correlation with the total surface gas density (HI+H_2), in particular the suggested law is that of eq. (1.5).

In the observed gas distributions differences between field and cluster spirals are found in the sense that cluster spirals have less gas, probably as a consequence of stronger interactions with the environment.Integrated colors of spiral galaxies (Josey & Arimoto 1992; Jimenez et al. 1998; Prantzos & Boissier 2000) indicate inside-out formation, as also found for the milky Way.

As an example of abundance gradients in a spiral galaxy we show in Figure 2.7 the observed and predicted gas distribution and abundance gradients for the disk of M101. In this case the gas distribution and the abundance gradients are reproduced with systematically smaller timescales for the disk formation relative to the MW (M101 formed faster), and the difference between the timescales of formation of the internal and external regions is smaller ($\tau_{M101} = 0.75R - 0.5$ Gyr, Chiappini et al. 2003a)

To conclude this section we like to recall a paper by Boissier et al. (2001) where a detailed study of the properties of disks is presented. They conclude that more massive disks are redder, more metal rich and more gas-poor than smaller ones. On the other hand their estimated SF efficiency (defined as the SFR per unit mass of gas) seem to be similar among different spirals: this leads them to conclude that more massive disks are older than less massive ones.

1.2.6 How to model the Hubble Sequence

The Hubble Sequence can be simply thought as a sequence of objects where the SFR proceeds faster in the early than in the late types (see also Sandage, 1986).

We take the Milky Way galaxy, whose properties are best known, as a

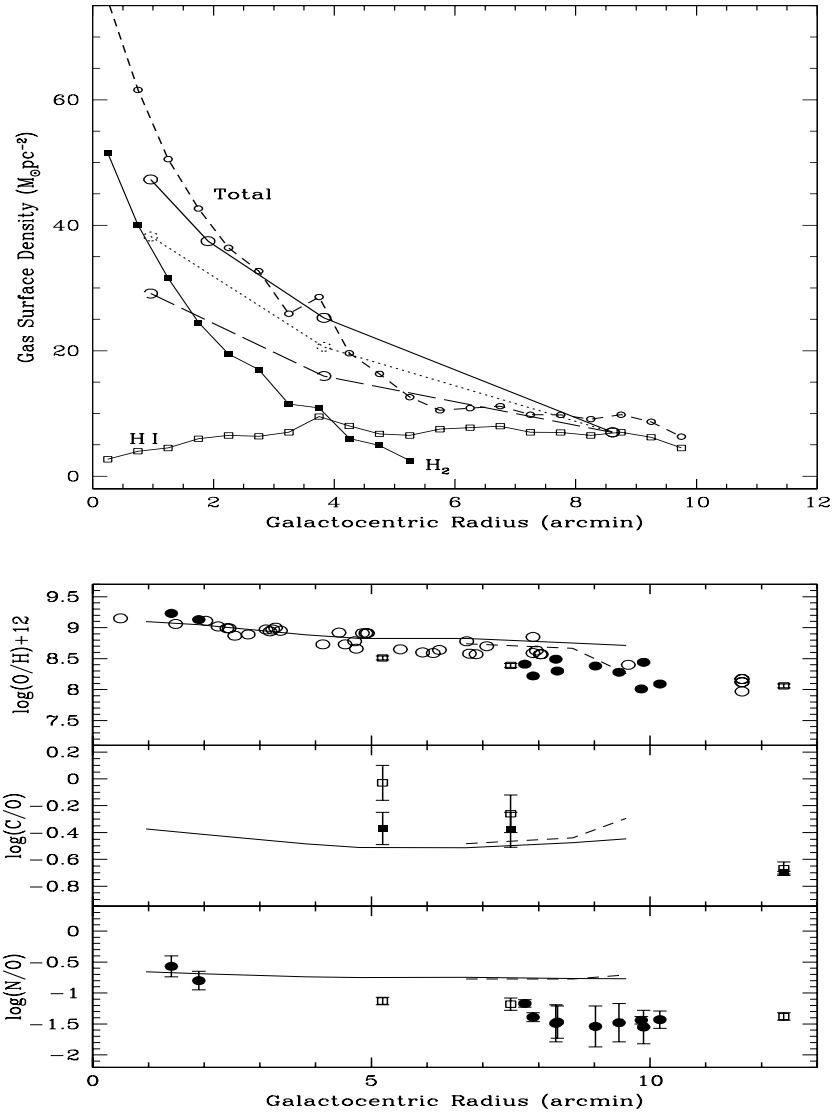

Fig. 1.7. Upper panel: predicted and observed gas distribution along the disk of M101. The observed HI, H_2 and total gas are indicated in the Figure. The large open circles indicate the models: in particular, the open circles connected by a continuous line refer to a model with central surface mass density of $1000 M_\odot pc^{-2}$, while the dotted line refers to a model with $800 M_\odot pc^{-2}$ and the dashed to a model with $600 M_\odot pc^{-2}$. Lower panel: predicted and observed abundance gradients of C,N,O elements along the disk of M101.The models are the lines and differ for a different threshold density for SF, being larger in the dashed model. All the models are by Chiappini et al. (2003a).

reference galaxy and we change the SFR relatively to the Galactic one, for which we adopt eq. (1.6). The quantity ν in eq. (1.6) is the efficiency of SF which we assume to be characteristic of each Hubble type. In the two-infall model for the Milky Way we adopt $\nu_{halo} = 2.0 Gyr^{-1}$ and $\nu_{disk} = 1.0 Gyr^{-1}$ (see Figure 2.1). The choice of adopting a dependence on the total surface mass density for the Galactic disk is due to the fact that it helps in producing a SFR strongly varying with the galactocentric distance, as required by the observed SFR and gas density distribution as well as by the abundance gradients. In fact, the inside-out scenario influences the rate at which the gas mass is accumulated by infall at each galactocentric distance and this in turn influences the SFR.

For bulges and ellipticals we assume that the SF proceeds like in a burst with very high star formation efficiency, namely:

$$SFR = \nu \sigma^k \tag{1.26}$$

with $k = 1.0$ for the sake of simplicity; $\nu = 10 - 20 Gyr^{-1}$ (see Matteucci, 1994; Pipino & Matteucci 2004).

For irregular galaxies, on the other hand, we assume that the SFR proceeds more slowly and less efficiently that in the Milky Way disk, in particular we assume the same SF law as for spheroids but with $0.01 \leq \nu(Gyr^{-1}) \leq 0.1$. Among irregular galaxies, a special position is taken by the Blue Compact Galaxies (BCG) namely galaxies which have blue colors as a consequence of the fact that they are forming stars at the present time, have small masses, large amounts of gas and low metallicities. For these galaxies, we assume that they suffered on average from 1 to 7 short bursts, with the SF efficiency mentioned above (see Bradamante et al. 1998 and next Lecture).

Finally, dwarf spheroidals are also a special cathegory, characterized by old stars, no gas and low metallicities. For these galaxies we assume that they suffered one long starburst lasting 7-8 Gyr or at maximum a couple of extended SF periods, in agreement with their measued Color-Magnitude diagram. It is worth noting that both ellipticals and dwarf spheroidals should loose most of their gas and therefore one may conclude that galactic winds should play an important role in their evolution, although ram pressure stripping cannot be excluded as a mechanism for gas removal. Also for these galaxies we assume the previous SF law with $k = 1$ and $\nu = 0.01 - 1.0 Gyr^{-1}$. Lanfranchi & Matteucci, (2003, 2004) developed more detailed models for dwarf spheroidals by adopting the SF history suggested by the Color-Magnitude diagrams of

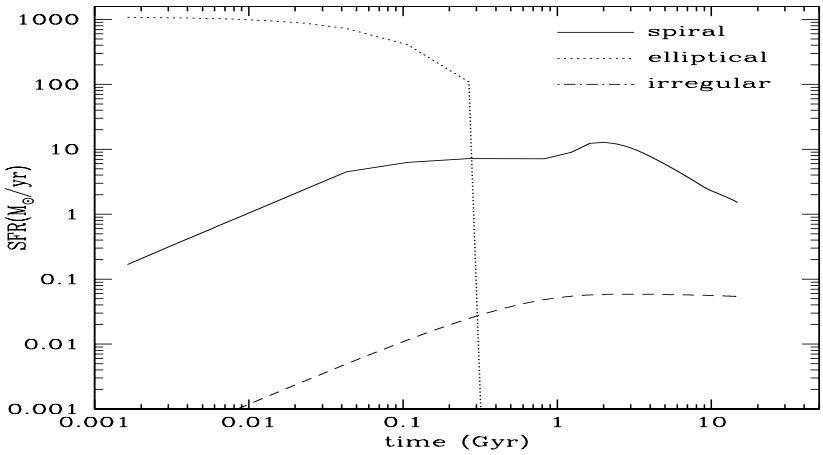

Fig. 1.8. Predicted SFRs in galaxies of different morphological type. Figure from Calura (2004). Note that for the elliptical galaxy the SF stops abruptly as a consequence of the galactic wind.

single galaxies and with the same efficiency of SF as above. In Figure 2.8 we show the adopted SFRs in different galaxies and in Figure 2.9 the corresponding predicted Type Ia SN rates. For the irregular galaxy, the predicted Type Ia SN rate refers to a specific galaxy, LMC, with a SFR taken from observations (see Calura et al. 2003) with an early ans a late burts of SF and low SF in between.

1.2.7 Type Ia SN rates in different galaxies

Following Matteucci & Recchi (2001) we define the typical timescale for Type Ia SN enrichment as *the time when the SN rate reaches the maximum*. In the following we will always adopt the SDS for the progenitors of Type Ia SNe. A point that is not often understood is that this timescale depends upon the progenitor lifetimes, IMF and SFR and therefore is not universal. Sometimes in the literature the typical Type Ia SN timescale is quoted as being universal and equal to 1 Gyr, whereas this is just the timescale at which the Type Ia SNe start to be important in the process of Fe enrichment in the solar vicinity.

Matteucci & Recchi (2001) showed that for an elliptical galaxy or a bulge of spiral with a high SFR the timescale for Type Ia SN enrichment

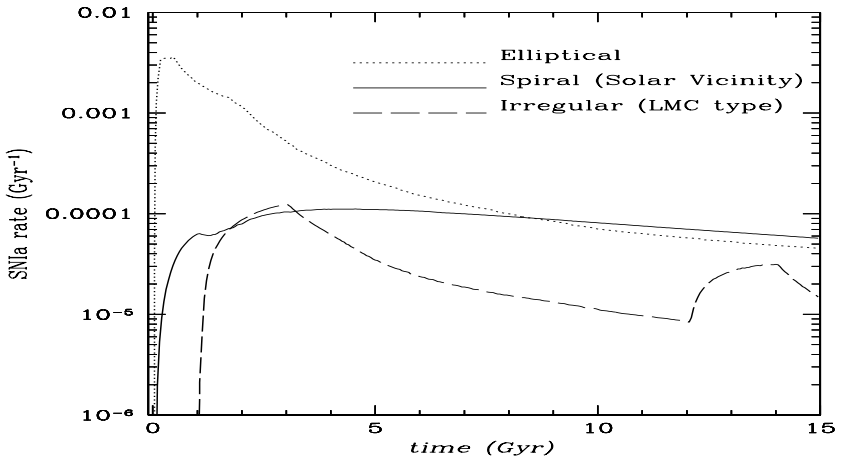

Fig. 1.9. Predicted Type Ia SN rates for the SFRs of Figure 2.8. Figure from Calura (2004). Note that for the irregular galaxy here the predictions are for the LMC, where a recent SF burst is assumed.

is quite short, in particular $t_{SNIa} = 0.3 - 0.5$ Gyr. For a spiral like the Milky Way, in the two-infall model, a first peak is reached at 1.0-1.5 Gyr (the time at which SNeIa become important as Fe producers (Matteucci and Greggio 1986) while a second less important peak occurs at $t_{SNIa} = 4 - 5$ Gyr. For an irregular galaxy with a continuous but very low SFR the timescale is $t_{SNIa} > 5$ Gyr.

1.2.8 Time-delay model for different galaxies

As we have already seen, the time-delay between the production of oxygen by Type II SNe and that of Fe by Type Ia SNe allows us to explain the [X/Fe] vs. [Fe/H] relations in an elegant way. However, the [X/Fe] vs. [Fe/H] plots depend not only on nucleosynthesis and IMF but also on other model assumptions, such as the SFR, through the absolute Fe abundance ([Fe/H]). Therefore, we should expect a different behaviour in galaxies with different SF histories. In Figure 2.10 we show the predictions of the time-delay model for a spheroid like the Bulge, for the solar vicinity and for a typical irregular magellanic galaxy.

As one can see in this Figure, we predict a long plateau, well above the solar value, for the [α/Fe] ratios in the Bulge (and ellipticals), owing

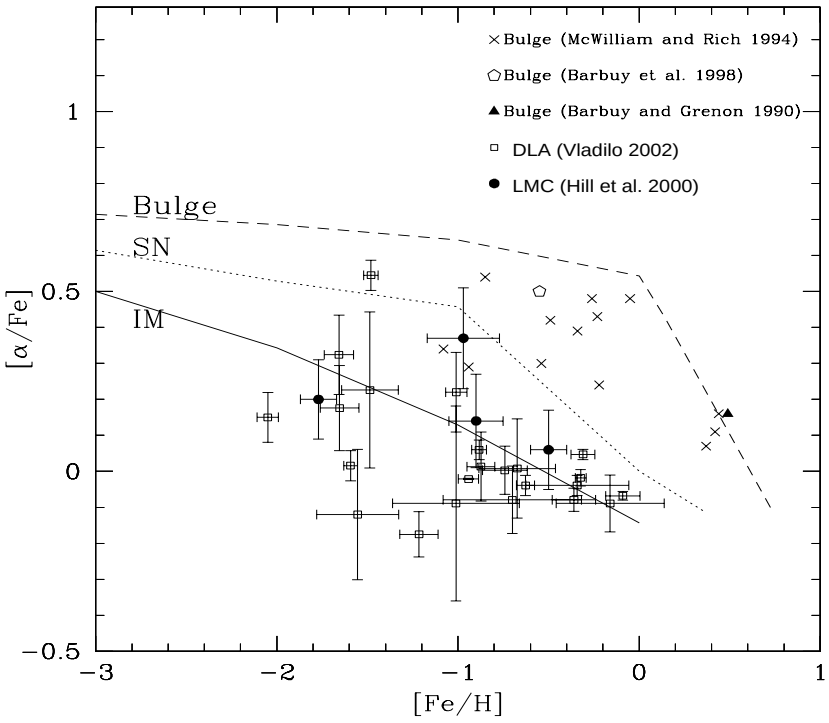

Fig. 1.10. Predicted [α/Fe] ratios in galaxies with different SF histories. The top line represents the predictions for the Bulge or for an elliptical galaxy of the same mass ($\sim 10^{10} M_{\odot}$), the median line represents the prediction for the solar vicinity and the lower line the prediction for an irregular magellanic galaxy. The differences among the various models are in the efficiency of star formation, being quite high for spheroids ($\nu = 20 Gyr^{-1}$), moderate for the Milky Way ($\nu = 1 - 2 Gyr^{-1}$) and low for irregular galaxies ($\nu = 0.1 Gyr^{-1}$). The nucleosynthesis prescriptions are the same in all objects. The time-delay between the production of α-elements and Fe, coupled with the different SF histories produces the differences in the plots. Data for Damped-Lyman-α systems, LMC and Bulge are shown for comparison.

to the fast Fe enrichment reached in these systems by means of Type II SNe: when the Type Ia SNe start enriching substantially the ISM, at 0.3-0.5 Gyr, the gas Fe abundance is already solar. The opposite occurs in Irregulars where the Fe enrichment proceeds very slowly so that when Type Ia SNe start restoring the Fe in a substantial way (> 3 Gyr) the Fe in the gas is still well below solar. Therefore, here we observe a steeper

slope for the [α/Fe] ratio. In other words, we have below solar [α/Fe] ratios at below solar [Fe/H] ratios. This diagram is very important since it allows us to recognize a galaxy type only by means of its abundances, and therefore it can be used to understand the nature of high redshift objects.

1.3 Lecture III: interpretation of abundances in dwarf irregulars

They are rather simple objects with low metallicity and large gas content, suggesting that they are either young or have undergone discontinuous star formation activity (bursts) or a continuous but not efficient star formation. They are very interesting objects for studying galaxy evolution. In fact, in "bottom-up" cosmological scenarios they should be the first self- gravitating systems to form and they could also be important contributors to the population of systems giving rise to QSO-absorption lines at high redshift (see Matteucci et al. 1997 and Calura et al. 2002).

1.3.1 Properties of Dwarf Irregular Galaxies

Among local star forming galaxies, sometimes referred to as HII galaxies, most are dwarfs. Dwarf irregular galaxies can be divided into two categories: Dwarf Irregular (DIG) and Blue Compact galaxies (BCG). These latter have very blue colors due to active star formation at the present time.

Chemical abundances in these galaxies are derived from optical emission lines in HII regions. Both DIG and BCG show a distinctive spread in their chemical properties, altough this spread is decreasing with the new more accurate data, but also a definite mass-metallicity relation.

From the point of view of chemical evolution, Matteucci and Chiosi (1983) first studied the evolution of DIG and BCG by means of analytical chemical evolution models including either outflow or infall and concluded that: closed-box models cannot account for the Z-log G($G = M_{gas}/M_{tot}$) distribution even if the number of bursts varies from galaxy to galaxy and suggested possible solutions to explain the observed spread. In other words, the data show a range of values of the metallicity for a given G ratio, and this means that the effective yield is lower than that of the Simple Model and vary from galaxy to galaxy.

The possible solutions suggested to lower the effective yield were:

- a. different IMF's
- b. different amounts of galactic wind
- c. different amounts of infall

In Figure 3.1 we show graphically the solutions a), b) and c). Concerning the solution a), one simply varies the IMF, whereas solutions b) and c) have been already descibed (eqs. 1.21 ans 1.23).

Later on, Pilyugin (1993) forwarded the idea that the spread observed also in other chemical properties properties of these galaxies such as in the He/H vs. O/H and N/O vs. O/H relations, can be due to self-pollution of the HII regions, which do not mix efficiently with the surrounding medium, coupled with "enriched" or "differential" galactic winds, namely different chemical elements are lost at different rates. Other models (Marconi et al. 1994; Bradamante et al. 1998) followed the suggestions of differential winds and introduced the novelty of the contribution to the chemical enrichment and energetics of the ISM by SNe of different type (II, Ia and Ib).

Another important feature of these galaxies is the mass-metallicity relation.

The existence of a luminosity-metallicity relation in irregulars and BCG was suggested first by Lequeux et al. (1979), then confirmed by Skillman et al. (1989) and extended also to spirals by Garnett & Shields (1987). In particular, Lequeux et al. suggested the relation:

$$M_T = (8.5 \pm 0.4) + (190 \pm 60)Z \tag{1.27}$$

with Z being the global metal content. Recently, Tremonti et al. (2004) analyzed 53000 local star-forming galaxies in the SDSS (irregulars and spirals). Metallicity was measured from the optical nebular emission lines. Masses were derived from fitting spectral energy distribution (SED) models. The strong optical nebular lines of elements other than H are produced by collisionally excited transitions. Metallicity was then determined by fitting simultaneously the most prominent emission lines ([OIII], H_β, [OII], H_α, [NII], [SII]). Tremonti et al. (2004) derived a relation indicating that 12+log(O/H) is increasing steeply from M_* going from $10^{8.5}$ to $10^{10.5}$ but flattening for $M_* > 10^{10.5}$.

In particular, the Tremonti et al. relation is:

$$12 + log(O/H) = -1.492 + 1.847(logM_*) - 0.08026(logM_*)^2. \tag{1.28}$$

This relation extends to higher masses the mass-metallicity relation

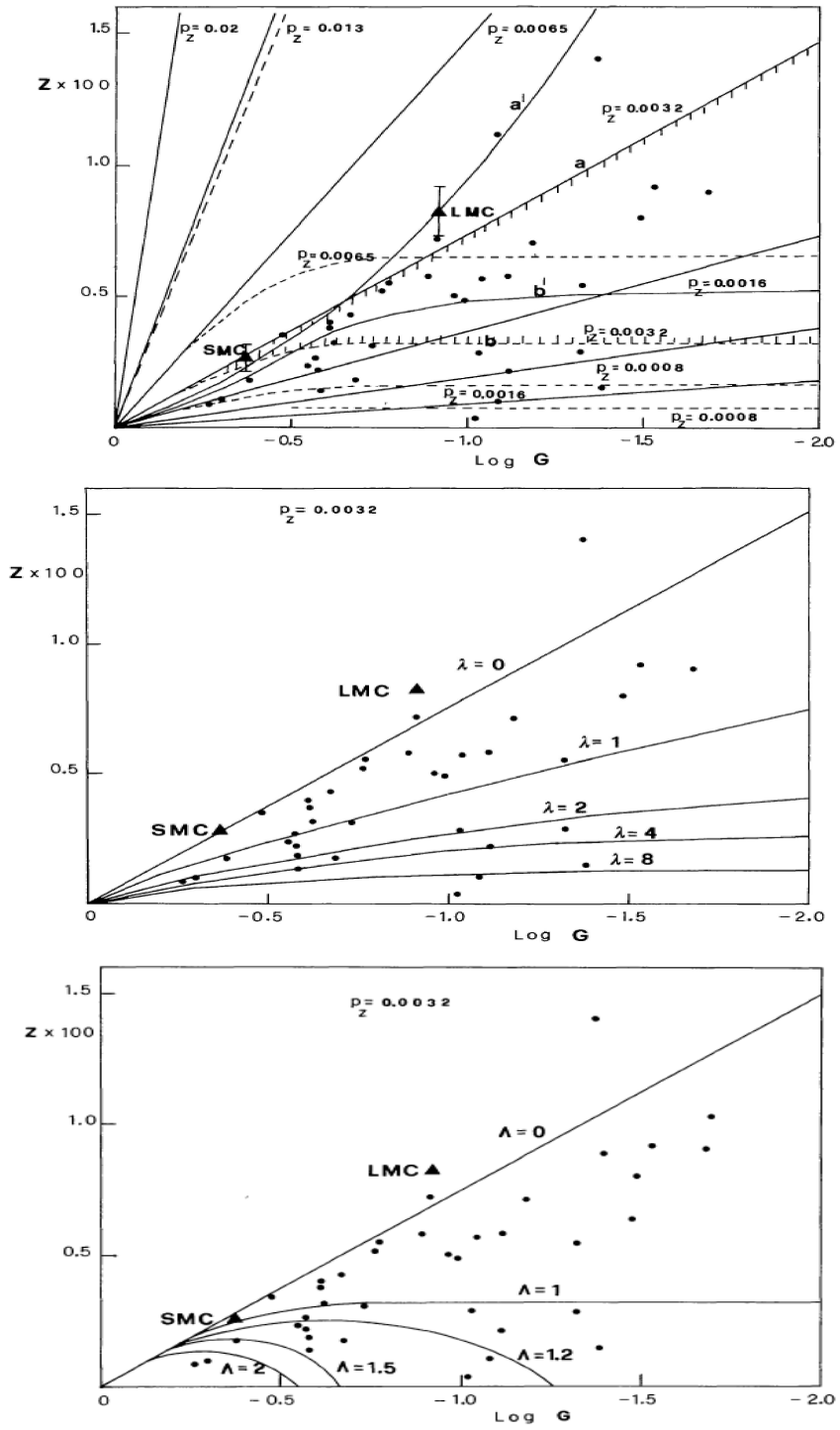

Fig. 1.11. The Z-*logG* diagram.Solutions a), b) and c) from top to bottom, to lower the effective yield in DIG and BCG by Matteucci & Chiosi (1983). Solution a) consists in varying the yield per stellar generation, here indicated by p_Z, just by changing the IMF. The solution b) and c) correspond to eqs. (1.21) and (1.23), respectively.

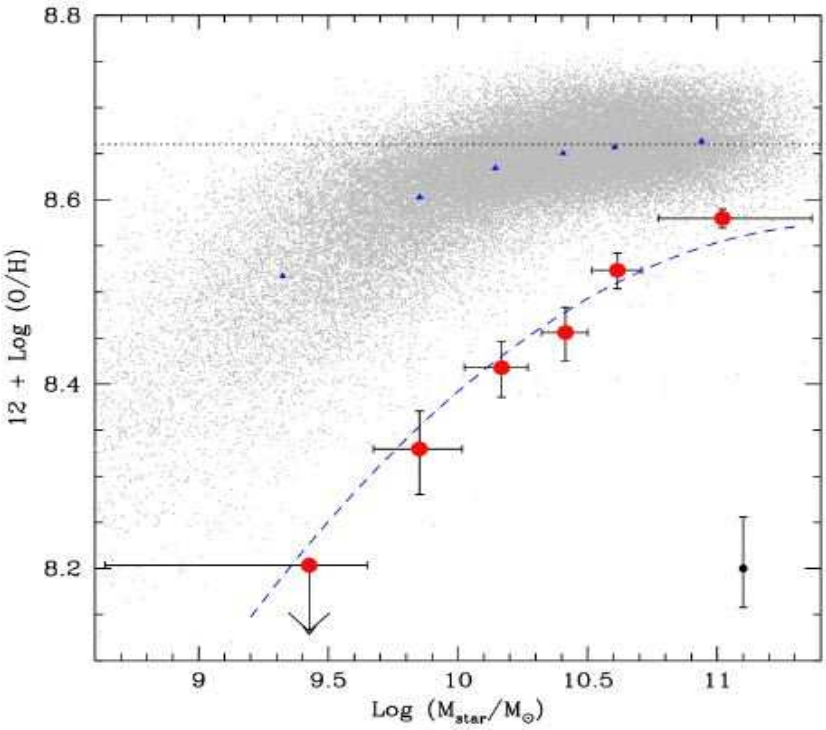

Fig. 1.12. Figure 3 from Erb et al. (2006) showing the mass-metallicity relation for star forming galaxies at high redshift. The data from Tremonti et al. (2004) are also shown.

found for star forming dwarfs and contains very important information on the physics governing galactic evolution. Even more recently, Erb et al. (2006) found the same mass-metallicity relation for star-forming galaxies at redshift z>2, with an offset from the local relation of ~ 0.3 dex. They used H_α and [NII] spectra. In Figure 3.2 we show the figure from Erb et al. (2006) for the mass-metallicity relation at high redshift which includes the relation of Tremonti et al. (2004) for the local mass-metallicity relation.

The most simple interpretation of the mass-metallicity relation is that the effective yield increases with galactic mass. This can be achieved in several ways, as shown in Fig. 3.1.: either by changing the IMF or the stellar yields as a function of galactic mass, or by assuming that the

galactic wind is less efficient in more massive systems, or that the infall rate is less efficient in more massive systems. One of the most common interpretations of the mass-metallicity relation is that the effective yield changes because of the occurrence of galactic winds, which should be more important in small systems. Evidences for galactic winds exist for dwarf irregular galaxies, as we will see next.

1.3.2 Galactic Winds

Papaderos et al. (1994) estimated a galactic wind flowing at a velocity of 1320 Km/sec for the irregular dwarf VIIZw403. The escape velocity estimated for this galaxy is $\simeq$ 50 Km/sec. Lequeux et al. (1995) suggested a galactic wind in Haro2=MKn33 flowing at a velocity of $\simeq 200 Km/sec$, also larger that the escape velocity of this object. More recently, Martin (1996;1998) found also supershells in 12 dwarfs, including IZw18, which imply gas outflow. Martin (1999) concluded that the galactic wind rates are several times the SFR. Finally, the presence of metals in the ICM (revealed by X-ray observations) and in the IGM (Ellison et al. 2000) represents a clear indication of the fact that galaxies lose their metals. However, we cannot exclude that the gas with metals is lost also by ram pressure stripping, especially in galaxy clusters.

In models of chemical evolution of dwarf irregulars (e.g. Bradamante et al. 1998) the feedback effects are taken into account and the condition for the development of a wind is:

$$(E_{th})_{ISM} \geq E_{Bgas} \tag{1.29}$$

namely, that the thermal energy of the gas is larger or equal to its binding energy. The thermal energy of gas due to SN and stellar wind heating is:

$$(E_{th})_{ISM} = E_{th_{SN}} + E_{th_w} \tag{1.30}$$

with the contribution of SNe being:

$$E_{th_{SN}} = \int_0^t \epsilon_{SN} R_{SN}(t^{'}) dt^{'}, \tag{1.31}$$

while the contribution of stellar winds is:

$$E_{th_w} = \int_0^t \int_{12}^{100} \varphi(m)\psi(t^{'})\epsilon_w dm dt^{'} \tag{1.32}$$

with $\epsilon_{SN} = \eta_{SN}\epsilon_o$ and $\epsilon_o = 10^{51}$erg (typical SN energy), and $\epsilon_w =$

$\eta_w E_w$ with $E_w = 10^{49}$erg (typical energy injected by a $20 M_\odot$ star taken as representative). η_w and η_{SN} are two free parameters and indicate the efficiency of energy transfer from stellar winds and SNe into the ISM, respectively, quantities still largely unknown. The total mass of the galaxy is expressed as $M_{tot}(t) = M_*(t) + M_{gas}(t) + M_{dark}(t)$ with $M_L(t) = M_*(t) + M_{gas}(t)$ and the binding energy of gas is:

$$E_{Bgas}(t) = W_L(t) + W_{LD}(t) \tag{1.33}$$

with:

$$W_L(t) = -0.5G\frac{M_{gas}(t)M_L(t)}{r_L} \tag{1.34}$$

which is the potential well due to the luminous matter and with:

$$W_{LD}(t) = -Gw_{LD}\frac{M_{gas}(t)M_{dark}}{r_L} \tag{1.35}$$

which represents the potential well due to the interaction between dark and luminous matter, where $w_{LD} \sim \frac{1}{2\pi}S(1 + 1.37S)$, with $S = r_L/r_D$, being the ratio between the galaxy effective radius and the radius of the dark matter core. The typical model for a BCG has a luminous mass of $10^8 - 10^9 M_\odot$, a dark matter halo ten times larger than the luminous mass and various values for the parameter S. The galactic wind in these galaxies develops easily but it carries out mainly metals so that the total mass lost in the wind is small.

1.3.3 Results on DIG and BCG from purely chemical models

Purely chemical models (Bradamante et al. 1998, Marconi et al. 1994) for DIG and BCG have been computed in the last years by varying the number of bursts, the time of occurrence of bursts t_{burst}, the star formation efficiency, the type of galactic wind (differential or normal), the IMF and the nucleosynthesis prescriptions. The best model of Bradamante et al. (1998) suggests that the number of bursts should be $N_{bursts} \leq 10$, the SF efficiency should vary from 0.1 to 0.7 Gyr^{-1} for either Salpeter or Scalo (1986) IMF (Salpeter IMF is favored). Metal enriched winds are favored. The results of these models also suggest that SNe of Type II dominate the chemical evolution and energetics of these galaxies, whereas stellar winds are negligible. The predicted [O/Fe] ratios tend to be overabundant relative to the solar ratios, owing to the predominance of Type II SNe during the bursts, in agreement with observational data

(see Figure 3.5 upper panel). Models with strong differential winds and N_{burst}=10 - 15 can however give rise to negative [O/Fe] ratios. The main difference between DIGs and BCGs, in these models, is that the BCGs suffer a present time burst, whereas the DIGs are in a quiescent phase.

In Figure 3.3 we show some of the results of Bradamante et al. (1998) compared with data on BCGs: it is evident from the Figure that the spread in the chemical properties can be simply reproduced by different SF efficiencies, which translate into different wind efficiencies.

In Fig 3.4 we show the results of the chemical evolution models of Henry et al. (2000). These models take into account exponential infall but not outflow. They suggested that the SF efficiency in extragalactic HII regions must have been low and that this effect coupled with the primary N production from intermediate mass stars can explain the plateau in log(N/O) observed at low 12+log(O/H). Henry et al. (2000) also concluded that ^{12}C is mainly produced in massive stars (yields by Maeder 1992) whereas ^{14}N is mainly produced in intermediate mass stars (yields by HG97). This conclusion, however, should be tested also on the abundances of stars in the Milky Way, where the flat behaviour of [C/Fe] vs. [Fe/H] from [Fe/H] =-2.2 up to [Fe/H]=0 suggest a similar origin for the two elements, namely partly from massive stars and mainly from low and intermediate mass ones (Chiappini et al. 2003b).

Concerning the [O/Fe] ratios we show results from Thuan et al. (1995) in Figure 3.5, where it is evident that generally BCGs have overabundant [O/Fe] ratios.

Very recently, an extensive study from SDSS of chemical abundances from emission lines in a sample of 310 metal poor emission line galaxies appeared (Izotov et al. 2006). The global metallicity in these galaxies ranges from $\sim 7.1(Z_{\odot}/30)$ to $\sim 8.5(0.7Z_{\odot})$. The SDSS sample is merged with 109 BCGs containing extremely low metallicity objects. These data, shown in Figure 3.5 lower panel, substantially confirm previous ones, showing how α-elements do not depend on the O abundance suggesting a common origin for these elements in stars with $M > 10M_{\odot}$, except for a slight increase of Ne/O with metallicity which is interpreted as due to a moderate dust depletion of O in metal rich galaxies. An important finding is that all the studied galaxies are found to have $\log(N/O) > -1.6$, which indicates that none of these galaxies is a truly young object, unlike the DLA systems at high redshift which show a $\log(N/O) \sim -2.3$.

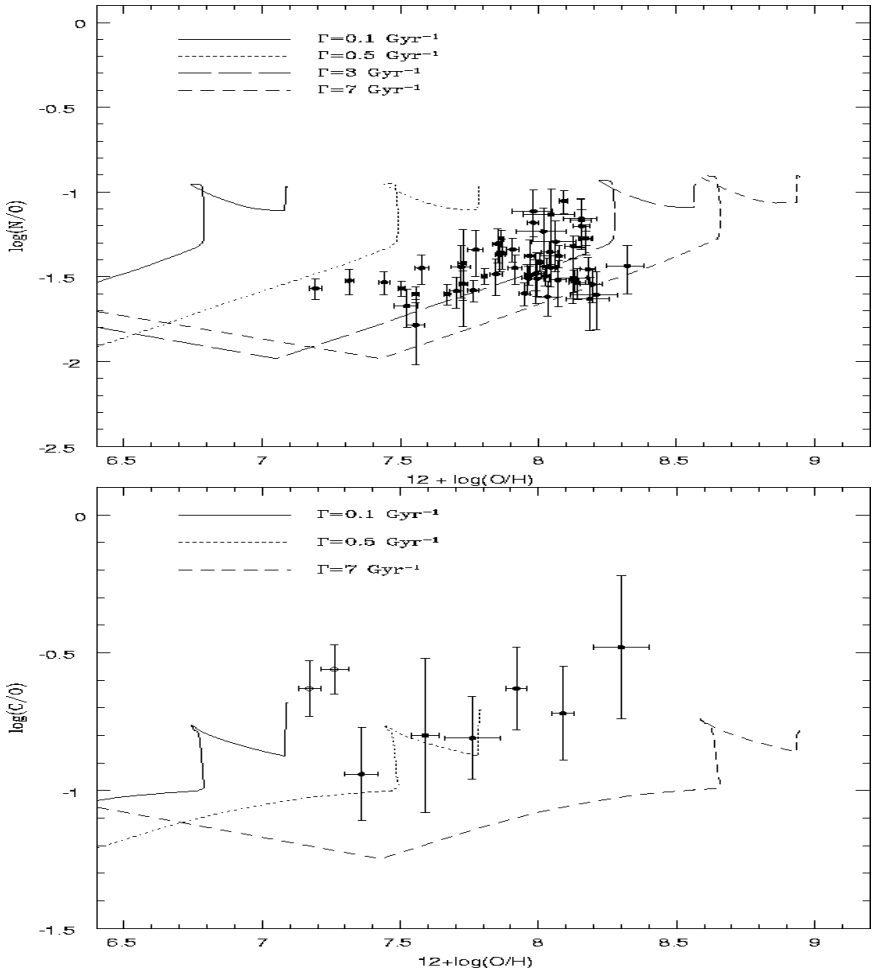

Fig. 1.13. Upper panel : predicted Log(N/O) vs. 12 + log(O/H) for a model with 3 bursts of SF separated by quiescent periods and different SF efficiencies here indicated with $\gamma = \nu$. Lower panel: predicted log(C/O) vs. 12 + log(O/H). The data in both panels are from Kobulnicky and Skillman (1996). The models assume a dark matter halo ten times larger than the luminous mass and S=0.3 (Bradamante et al. 1998, see text).

1.3.4 Results from Chemo-Dynamical models: IZw18

IZw18 is the most metal poor local galaxy, thus resembling to a primordial object. Probably it did not experience more than two bursts of star formation including the present one. The age of the oldest stars

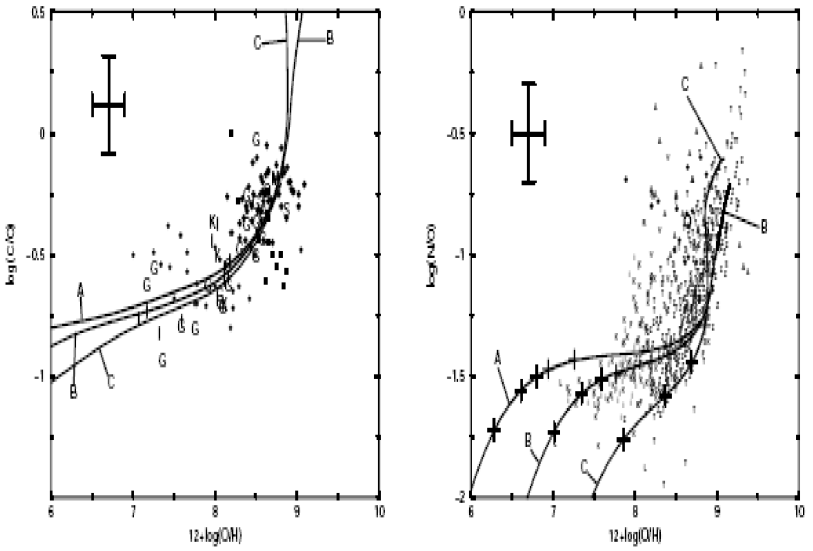

Fig. 1.14. Figure from Henry et al. (2000): a comparison between numerical models and data for extragalactic HII regions and stars (filled circles, filled boxes and filled diamonds); M and S mark the position of the Galactic HII regions and the Sun, respectively. Their best model is model B with an efficiency of SF of $\nu = 0.03$.

in this galaxy is still uncertain, although recently Tosi et al. (2006) suggested an age possibly $>$ 2 Gyr. The oxygen abundance in IZW18 is 12+log(O/H)= 7.17-7.26, $\sim$ 15-20 times lower than the solar oxygen (12+ log(O/H)= 8.39, Asplund et al. 2005) and log N/O= -1.54/ -1.60 (Garnett et al. 1997).

Recently, FUSE provided abundances also for HI in IZw18: the evidence is that the abundances in the HI are lower than in the HII (Aloisi et al. 2003; Lecavelier des Etangs et al. 2003). In particular, Aloisi et al. (2003) found the largest difference relative to the HII data.

Chemo-dynamical (2-D) models (Recchi et al. 2001) studied first the case of IZw18 with only one burst at the present time and concluded that the starburst triggers a galactic outflow. In particular, the metals leave the galaxy more easily than the unprocessed gas and among the enriched material the SN Ia ejecta leave the galaxy more easily than other ejecta. In fact, Recchi et al. (2001) had reasonably assumed that Type Ia SNe can transfer almost all of their energy to the gas, since

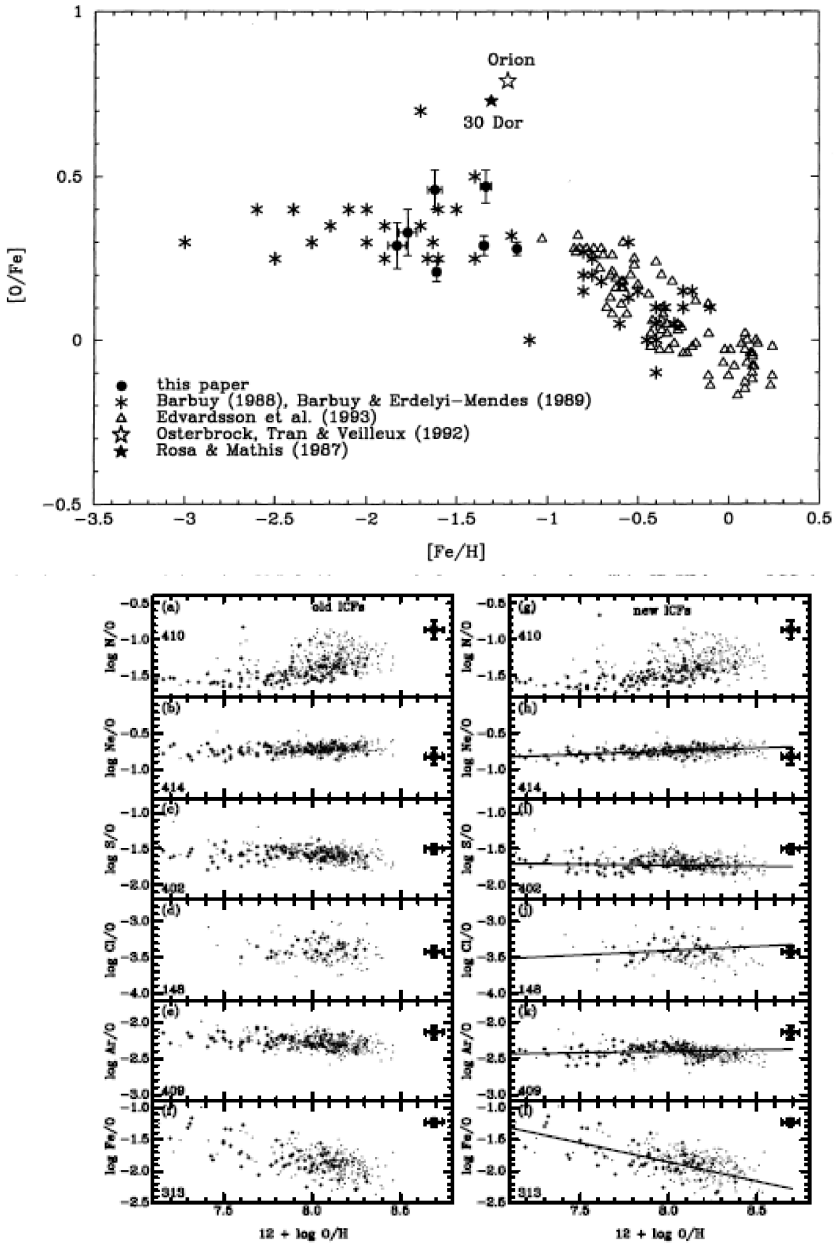

Fig. 1.15. Upper panel: [O/Fe] vs. [Fe/H] observed in a sample of BCGs by Thuan et al. (1995) (filled circles), open triangles and asterisks are disk and halo stars shown for comparison.Figure from Thuan et al. (1995). Lower panel: new data from Izotov et al. (2006). The large filled circles represent the BCGs whereas the dots are the SDSS galaxies. Abundances in the left panel are calculated as in Thuan et al. (1995) whereas those in the right panel are calculated as in Izotov et al. (2006) (see original papers for details). Figure from Izotov et al. (2006).

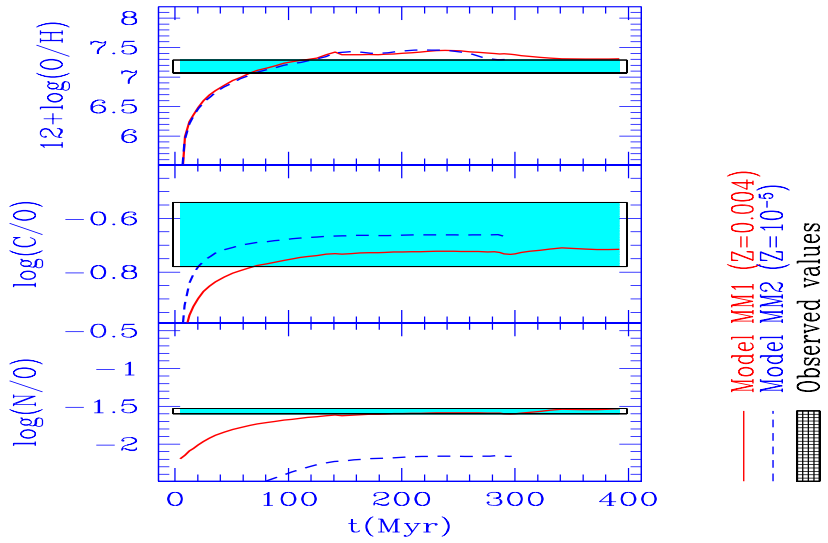

Fig. 1.16. Figure from Recchi et al. (2004): predicted abundances for the HII region in IZw18 (dashed lines represent a model adopting the yields of Meynet & Maeder (2002) for $Z = 10^{-5}$, whereas the continuous line refers to a higher metallicity (Z=0.004).Observational data are represented by the shaded areas.

they explode in an already hot and rarified medium after the SN II explosions. As a consequence of this, they predicted that the [α/Fe] ratios in the gas inside the galaxy should be larger than the [α/Fe] ratios in the gas outside the galaxy. At variance with previous studies, they found that most of the metals are already in the cold gas phase after 8-10 Myr since the superbubble does not break immediately and thermal conduction can act efficiently. In the following, Recchi et al. (2004) extended the model to a two-burst case, always with the aim of reproducing the characteristics of IZw18. The model well reproduces the chemical properties of IZw18 with a relatively long episode of SF lasting 270 Myr plus a recent burst of SF still going on. In Figure 3.6 we show the predictions of Recchi et al. (2004) for the abundances in the HII regions of IZW18 and in Figure 3.7 those for the HI region, showing a little difference between the HII and HI abundances, more in agreement with the data of Lecavelier des Etangs et al. (2004).

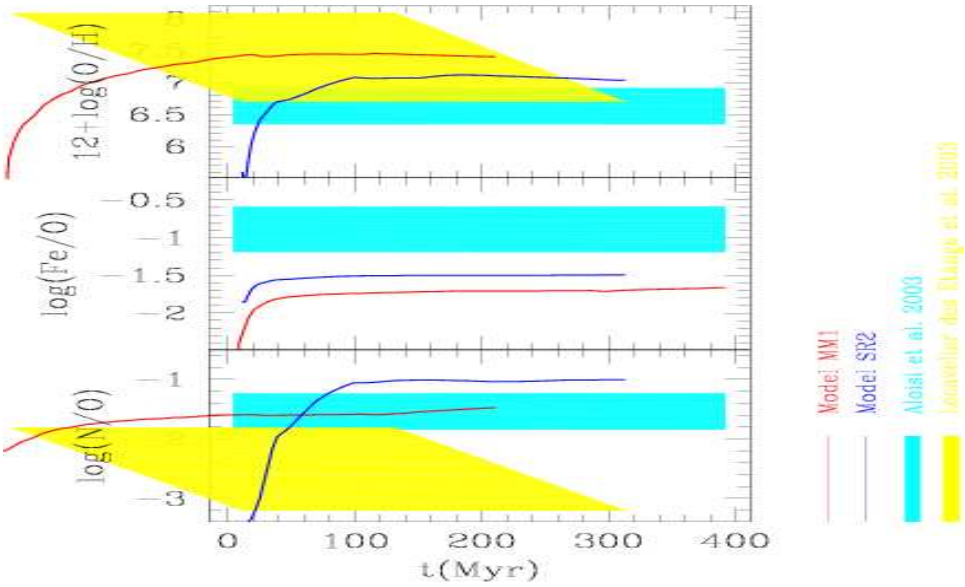

Fig. 1.17. Figure from Recchi et al. (2004): predicted abundances for the HI region. The models are the same as in Figure 3.6. Observational data are represented by the shaded areas. The upper shaded area in the panel for oxygen and the lower shaded area in the panel for N/O represent the data of Lecavelier des Etangs et al. (2003).

1.4 Lecture IV: Elliptical galaxies-Quasars- ICM Enrichment

1.4.1 Ellipticals

We recall here some of the most important properties of ellipticals or early type galaxies (ETG) which are systems made of old stars with no gas and no ongoing SF. The metallicity of ellipticals is measured only by means of metallicity indeces obtained from their integrated spectra which are very similar to those of K giants. In order to pass from metallicity indices to [Fe/H] one needs then to adopt a suitable calibration often based on population synthesis models (Worthey, 1994). We also summarize the most common scenarios for the formation of ellipticals.

1.4.2 Chemical Properties

The main properties of the stellar populations in ellipticals are:

- There exist the well-known Color-Magnitude and Color - σ_o (veloc-

ity dispersion) relations indicating that the integrated colors become redder with increasing luminosity and mass (Faber 1977; Bower et al. 1992). These relations are interpreted as a metallicity effect, although a well known degeneracy exists between metallicity and age of the stellar populations in the integrated colors (Worthey 1994).

- The index Mg_2 is normally used as a metallicity indicator since it does not depend much upon the age of stellar populations. There exists for ellipticals a well defined Mg_2–σ_o relation, equivalent to the already discussed mass-metallicity relation for star forming galaxies (Bender et al. 1993; Bernardi et al. 1998; Colless et al. 1999).
- Abundance gradients in the stellar populations inside ellipticals are found (Carollo et al. 1993; Davies et al. 1993). Kobayashi & Arimoto (1999) derived the average gradient for ETGs from a large compilation of data and this is: $\Delta[Fe/H]/\Delta r \sim -0.3$, with the average metallicity in ETGs of $< [Fe/H] >_* \sim -0.3$dex (from -0.8 to +0.3 dex).
- A very important characteristic of ellipticals is that their central dominant stellar population (dominant in the visual light) shows an overabundance, relative to the Sun, of the Mg/Fe ratio, $< [Mg/Fe] >_* > 0$ (from 0.05 to + 0.3 dex) (Peletier 1989; Worthey et al. 1992; Weiss et al. 1995; Kuntschner et al. 2001).
- In addition, the overabundance increases with increasing galactic mass and luminosity, $< [Mg/Fe] >_* vs. \sigma_o$, (Worthey et al. 1992; Matteucci 1994; Jorgensen 1999; Kuntschner et al. 2001).

1.4.3 Scenarios for galaxy formation

The most common ideas on the formation and evolution of ellipticals can be summarized as:

- they formed by an early monolithic collapse of a gas cloud or early merging of lumps of gas where dissipation plays a fundamental role (Larson 1974; Arimoto & Yoshii 1987; Matteucci & Tornambè 1987). In this model SF proceeds very intensively until a galactic wind is developed and SF stops after that. The galactic wind is devoiding the galaxy from all its residual gas.
- They formed by means of intense bursts of star formation in merging subsystems made of gas (Tinsley & Larson 1979). In this picture SF stops after the last burst and gas is lost via ram pressure stripping or galactic wind.

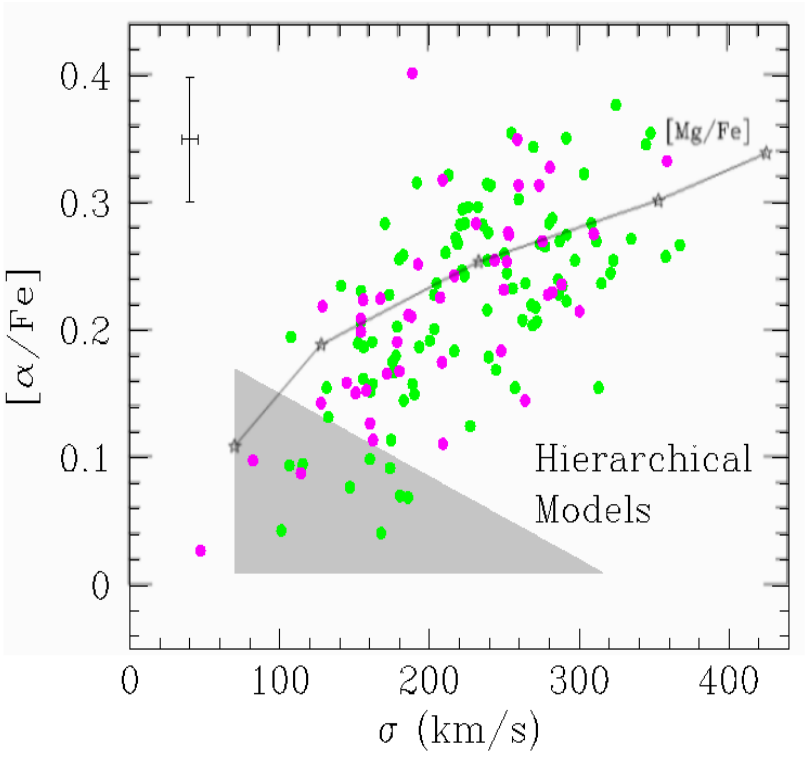

Fig. 1.18. The relation [α/Fe] vs. velocity dispersion (mass) for ETGs. Figure adapted from Thomas et al. (2002).The continuous line represents the prediction of the model by Pipino & Matteucci (2004). The shaded area represents the prediction of hierarchical models for the formation of ellipticals.The symbols are the observational data.

- They formed by early merging of lumps containing gas and stars in which some dissipation is present (Bender et al. 1993).
- They formed and continue to form in a wide redshift range and preferentially at late epochs by merging of early formed stellar (e.g. Kauffmann et al. 1993;1996).

Pipino & Matteucci (2004), by means of recent revised monolithic models taking into account the development of a galactic wind (see Lecture III), computed the relation [Mg/Fe] versus mass (velocity dispersion) and compared it with the data by Thomas et al. (2002). Thomas (1990) already showed how hierarchical semi-analitycal models cannot

reproduce the observed [Mg/Fe] vs. mass trend, since in this scenario massive ellipticals have longer periods of star formation than smaller ones. In Figure 4.1, the original figure from Thomas et al. (2002) is shown, where we have plotted also our predictions. In the Pipino & Matteucci (2004) model it is assumed that the most massive galaxies assemble faster and form stars faster than less massive ones. The adopted IMF is the Salpeter one. In other words, more massive ellipticals seem to be older than less massive ones, in agreement with what found for spirals (Boissier et al. 2001). In particular, in order to explain the observed $< [Mg/Fe] >_* > 0$ in giant ellipticals the dominant stellar population should have formed on a time scale no longer than 3-5 $\cdot 10^8$ yr (Weiss et al. 1995; Pipino & Matteucci 2004).

1.4.4 Ellipticals-Quasars connection

We know now that most if not all massive ETGs are hosting an AGN for sometime during their life. Therefore, there is a strict link between the quasar activity and the evolution of ellipticals.

1.4.5 The chemical evolution of QSOs

It is very interesting to study the chemical evolution of QSOs by means of the broad emission lines in the QSO region. The first studies by Wills et al. (1985) and Collin-Souffrin et al. (1986) found that the abundance of Fe in QSOs, as measured from broad emission lines, turned out to be $\sim$ a factor of 10 more than the solar one and this represented a challenge for chemical evolution model makers. Hamman & Ferland (1992) from N V/C IV line ratios in QSOs derived the N/C abundance ratios and inferred the QSO metallicities. They suggested that N is overabundant by factors of 2-9 in the high redshift sources ($z > 2$). Metallicities 3-14 times the solar one were also suggested in order to produce such a high N abundance, under the assumption of a mainly secondary N. To interpret their data they built a chemical evolution model, a Milky Way- like model, and suggested that these high metallicities are reached in only 0.5 Gyr, implying that QSOs are associated with vigourous star formation. At the same time, Padovani & Matteucci (1993) and Matteucci & Padovani (1993) proposed a model for QSOs in which QSOs are hosted by massive ellipticals. They assumed that after the occurrence of a galactic wind the galaxy evolves passively and that for massess $> 10^{11} M_\odot$ the gas restored by the dying stars is not lost but it feeds the central

black hole. They showed that in this context the stellar mass loss rate can explain the observed AGN luminosities. They also found that solar abundances in the gas are reached in no more than 10^8 years explaining in a natural way the standard emission lines observed in high-z QSOs. The predicted abundances could explain the data available at that time and solve the problem of the quasi-similarity of QSO spectra at different redshifts. Finally, they suggested also a criterium for establishing the ages of QSOs on the basis of the [α/Fe] ratios observed from broad emission lines (see also Hamman & Ferland 1993).

Much more recently, Maiolino et al. (2005, 2006) used more than 5000 QSO spectra from SDSS data to investigate the metallicity of the broad emission line region in the redshift range $2 < z < 4.5$ and over the luminosity range $-24.5 < M_B < -29.5$. They found substantial chemical enrichment in QSOs already at z = 6. Models for ellipticals by Pipino & Matteucci (2004) were used as a comparison with the data and they well reproduce the data, as one can see in Figure 4.2. In this Figure the evolution of the abundances of several chemical elements in the gas of a typical elliptical are shown. The elliptical suffers a galactic wind at around 0.4 Gyr since the beginning of star formation. This wind devoids the galaxy of all the gas present at that time. After this time, the SF stops and the galaxy evolves passively. All the gas restored after the galactic wind event by dying stars can in principle feed the central black hole, thus the abundances shown in Figure 4.2, after the time of the wind, can be compared with the abundances measured in the broad emission line region. As one can see, the predicted Fe abundance after the galactic wind is always higher than the O one, owing to the Type Ia SNe which continue to produce Fe even after the stop in the SF. On the other hand, O and α-elements stop to be produced when the SF halts. The comparison between the predicted abundances and those derived from the QSO spectra, are in very good agreement and indicates ages for these objects between 0.5 and 1 Gyr.

Finally, in the context of the joint formation of QSOs and ellipticals we recall the work of Granato et al. (2001) who includes the energy feedback from the central AGN in ellipticals. This feedback produces outflows and stops the SF in a down-sizing fashion, in agreement with the chemical properties of ETGs indicating a shorter period of SF for the more massive objects.

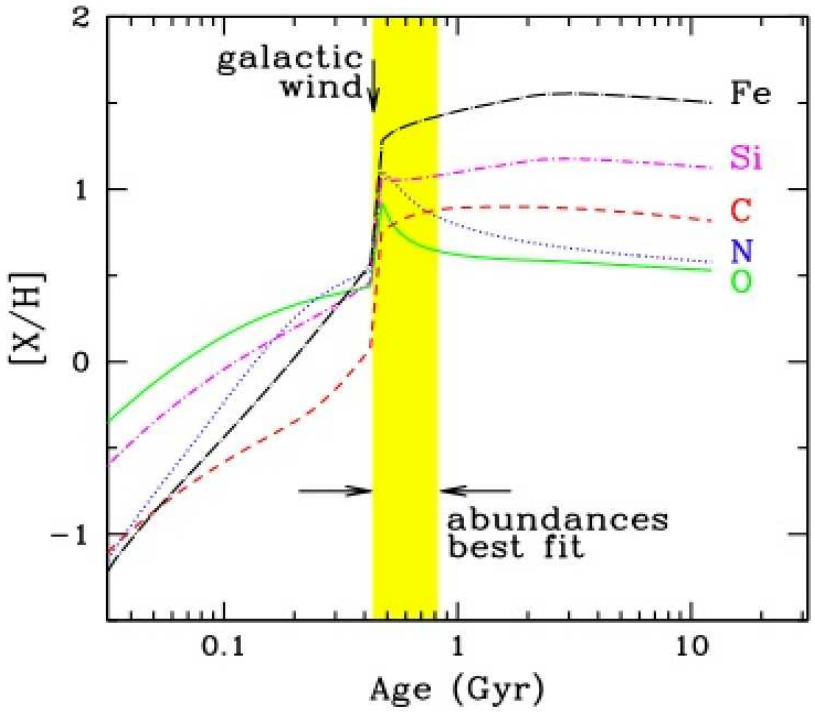

Fig. 1.19. The temporal evolution of the abundances of several chemical elements in the gas of an elliptical galaxy with luminous mass of $10^{11} M_{\odot}$. Feedback effects are taken into account in the model (Pipino & Matteucci 2004), as described in Lecture III. The downarrow indicates the time for the occurrence of the galactic wind. After this time, the SF stops and the elliptical evolves passively. All the abundances after the time for the occurrence of the wind are those that we observe in the broad emission line region region. The shaded area indicates the abundance sets which best fit the line ratios observed in the QSO spectra. Figure from Maiolino et al. 2006.

1.4.6 The chemical enrichment of the ICM

The X-ray emission from galay clusters is generally interpreted as thermal bremsstrahlung in a hot gas (10^7-10^8 K). There are several emission lines (O, Mg, Si, S) including the strong Fe K-line at around 7keV which was discovered by Mitchell et al. (1976). The iron is the best studied element in clusters. For $kT \geq 3$ keV the intracluster medium (ICM) Fe abundance is constant and $\sim 0.3 Fe_{\odot}$ in the central cluster regions;

the existence of metallicity gradients seems evident only in some clusters (see Renzini 2004). At lower temperatures, the situation is not so simple and the Fe abundance seems to increase. The first works on chemical enrichment of the ICM even preceeded the discovery of the Fe line (Gunn & Gott 1972, Larson & Dinerstein 1975). In the following years other works appeared such as those of Vigroux (1977), Himmes & Biermann (1988) and Matteucci & Vettolani (1988). In particular, Matteucci & Vettolani (1988) started a more detailed approach to the problem followed by David et al. (1991), Arnaud (1992), Renzini et al. (1993), Elbaz et al. (1995), Matteucci & Gibson (1995), Gibson & Matteucci (1997), Lowenstein & Mushotzky (1996), Martinelli et al. (2000), Chiosi (2000), Moretti et al. (2003). The majority of these papers assumed that galactic winds (mainly from ellipticals and S0 galaxies) are responsible for the ICM chemical enrichment. In fact, ETGs are the dominant type of galaxy in clusters and Arnaud (1992) found a clear correlation between the mass of Fe in clusters and the total luminosity of ellipticals. No such correlation was found for spirals in clusters. Alternatively, the abundances in the ICM are due to ram pressure stripping (Himmes & Biermann 1988) or derive from a chemical enrichment from pre-galactic Pop III stars (White & Rees 1978).

In Matteucci & Vettolani (1988) the Fe abundance in the ICM relative to the Sun, $X_{Fe}/X_{Fe_\odot}$, was calculated as $(M_{Fe})_{pred}/(M_{gas})_{obs}$ to be compared with the observed ratio $(X_{Fe}/X_{Fe_\odot})_{obs} = 0.3 - 0.5$ (Rothenflug & Arnaud 1985). They found a good agreement with the observed Fe abundance in clusters if all the Fe produced by ellipticals and S0, after SF has stopped, is eventually restored into the ICM and if the majority of gas in clusters has a primordial origin. Low values for [Mg/Fe] and [Si/Fe] were predicted at the present time, due to the short period of SF in ETGs and to the Fe produced by Type Ia SNe. With Salpeter IMF they found that the Type Ia SNe contribute $\geq 50\%$ of the total Fe in clusters. This leads to a bimodality in the [α/Fe] ratios in the stars and in the gas in the ICM, since the stars have overabundances of [α/Fe]> 0 whereas the ICM should have [α/Fe]≤ 0. The same conclusion was reached and more highlighted later by Renzini et al. (1993). More recently, Pipino et al. (2002) computed the chemical enrichment of the ICM as a function of redshift by considering the evolution of the cluster luminosity function and an updated treatment of the SN feedback. They adopted Woosley & Weaver (1995) yields for Type II SNe and Nomoto et al. (1997) W7 model for Type Ia SNe and a Salpeter IMF. They also predicted solar or undersolar [α/Fe] ratios in the ICM.

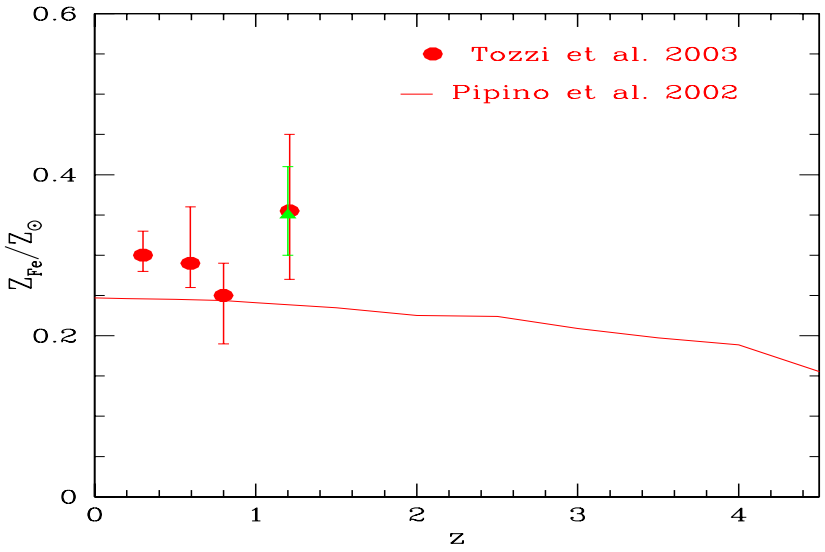

Fig. 1.20. Observed Fe abundance and predicted Fe abundance in the ICM as a function of redshift: data from Tozzi et al. (2003), model (continuous line) from Pipino et al. (2002), where the formation of ETGs was assumed to occur at z=8.

The observational data on abundance ratios in clusters are still uncertain and vary from cluster centers where they tend to be solar or undersolar to the outer regions where they tend to be oversolar (e.g. Tamura et al. 2004). So, no firm conclusions can be drawn on this point. Concerning the evolution of the Fe abundance in the ICM as a function of redshift, most of the above mentioned models predict very little or no evolution of the Fe abundance from z=1 to z=0 (Pipino et al. 2002). This prediction seemed to be in good agreement with data from Tozzi et al. (2003) as shown Figure. However, more recently, more data of Fe abundance for high redshift clusters appeared showing a different behaviour.

In Figure 4.4 we show the data of Balestra et al. (2006) who claim an increase, by at least a factor of two, of the Fe abundance in the ICM from z=1 to z=0. Clearly, if we assume that only ellipticals have contributed to the Fe abundance in the ICM, this effect is difficult to explain unless we assume recent star formation in ellipticals. Another possible explanation could be that spiral galaxies contribute to Fe when

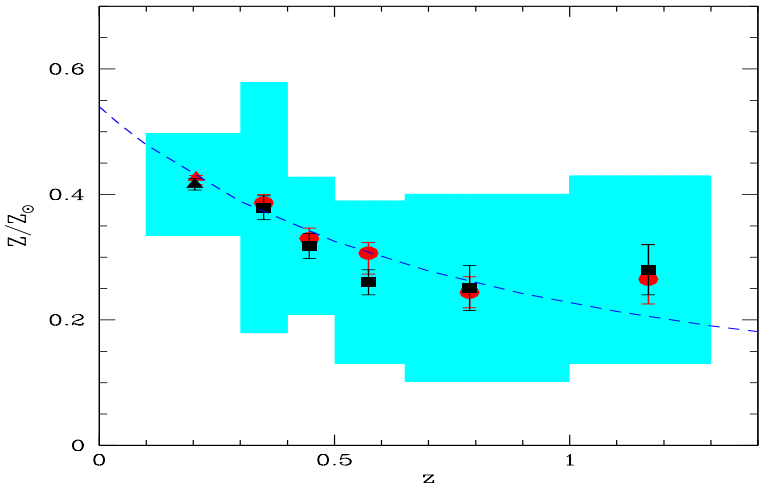

Fig. 1.21. New data (always relative to Fe) from Balestra et al. (2006) showing an increase of the Fe abundance in the ICM from z=1 to z=0. Error bars refer to 1σ confidence level. The big shaded area represents the rms dispersion. Figure from Balestra et al. (2006).

they become S0 as a consequence of ram pressure stripping, and this morphological transformation might have started just at z=1.

1.4.7 Conclusions on the enrichment of the ICM

From what said before we can conclude that:

- Elliptical galaxies are the dominant contributors to the abundances and energetic content of the ICM. A constant Fe abundance of $\sim 0.3 Fe_{\odot}$ is found in the central regions of clusters hotter than 3keV (Renzini 2004).
- Good models for the chemical enrichment of the ICM should reproduce the iron mass measured in clusters plus the [α/Fe] ratios inside galaxies and in the ICM as well as the Fe mass to light ratio (IMLR= $M_{Fe_{ICM}}/L_B$, with L_B being the total blue luminosity of member galaxies, as defined by Renzini et al. (1993). Abundance

ratios are very powerful tools to impose constraints on the evolution of ellipticals and of the ICM.

- Models which do not assume a top-heavy IMF for the galaxies in clusters (a Salpeter IMF can reproduce at best the properties of local ellipticals) predict $[\alpha/\mathrm{Fe}] > 0$ inside ellipticals and $[\alpha/\mathrm{Fe}] \leq 0$ in the ICM. Observed values are still too uncertain to draw firm conclusions on this point.

Acknowledgements

This research has been supported by INAF (Italian National Institute for Astrophysics), Project PRIN-INAF-2005-1.06.08.16

References

[1] Alibés, A., Labay, J. & Canal, R., 2001, A&A, 370, 1103
[2] Aloisi, A., Savaglio, S., Heckman, T. M., Hoopes, C. G., Leitherer, C. & Sembach, K. R., 2003, ApJ, 595, 760
[3] Argast, D., Samland, M., Gerhard, O.E. & Thielemann, F.-K., 2000, A&A 356, 873
[4] Arimoto, N. & Yoshii, Y. 1987, A&A 173, 23
[5] Arnaud, M., Rothenflug, R., Boulade, O.,Vigroux, L. & Vangioni-Flam, E., 1992, A&A, 254, 49
[6] Asplund, M., Grevesse, N. & Sauval, A.J., 2005, ASP (Astronomical Society of the Pacific) Conf. Series, Vol. 336, p.55
[7] Balestra, I., Tozzi, P., Ettori, S., Rosati, P., Borgani, S., Mainieri, V., Norman, C. & Viola, M., 2006, A&A in press, astro-ph/0609664
[8] Barbuy, B. & Grenon, M., 1990. in :Bulges of Galaxies, eds. B.J. Jarvis & D.M. Terndrup, ESO/CTO Workshop, p.83
[9] Barbuy, B.,Ortolani, S.& Bica, E., 1998, A&AS, 132, 333
[10] Bender, R., Burstein, D. & Faber, S. M., 1993, ApJ, 411, 153
[11] Berman, B.C. & Suchov, A.A., 1991, Astrophys. Space Sci. 184, 169
[12] Bernardi, M., Renzini, A., da Costa, L. N.., Wegner, G. & al., 1998, ApJ, 508, L143
[13] Boissier, S., Prantzos, N., 1999, MNRAS, 307, 857
[14] Boissier, S., Boselli, A., Prantzos, N. & Gavazzi, G., 2001, MNRAS, 321, 733
[15] Bradamante, F., Matteucci, F. & D'Ercole, A., 1998, A&A, 337, 338
[16] Calura, F. 2004 PhD Thesis, Trieste University
[17] Calura, F., Matteucci, F. & Vladilo, G., 2003, MNRAS, 340, 59
[18] Carollo, C. M., Danziger, I. J.& Buson, L., 1993, MNRAS, 265, 553
[19] Cayrel, R., Depagne, E., Spite, M., Hill, V., Spite, F., Franois, P., Plez, B., Beers, T., & al., 2004, A&A, 416, 117
[20] Chabrier, G., 2003, PASP, 115, 763
[21] Chang, R.X., Hou, J.L., Shu, C.G. & Fu, C.Q., 1999, A&A 350, 38
[22] Chiappini, C,. Hirschi, R., Meynet, G., Ekstroem, S., Maeder, A. & Matteucci, F., 2006, A&A, 449, L27
[23] Chiappini, C., Matteucci F. & Gratton R. 1997, ApJ, 477, 765
[24] Chiappini, C., Matteucci, F. & Meynet, G. 2003b, A&A, 410, 257
[25] Chiappini, C., Matteucci, F. & Padoan, P., 2000, ApJ, 528, 711
[26] Chiappini, C., Matteucci, F., & Romano, D., 2001, ApJ, 554, 1044

[27] Chiappini, C., Romano, D & Matteucci, F., 2003a, MNRAS, 339, 63
[28] Chiosi, C., 1980, A&A, 83, 206
[29] Chiosi, C., 2000, A&A 364, 423
[30] Colless, M., Burstein, D., Davies, R.L., McMahan, R. K., Saglia, R. P. & Wegner, G., 1999, MNRAS, 303, 813
[31] Collin-Souffrin, S., Joly, M., Pequignot, D. & Dumont, S., 1986, A&A, 166, 27
[32] Davies, R. L., Sadler, E. M. & Peletier, R. F., 1993, MNRAS, 262, 650
[33] David, L.P., Forman, W., & Jones, C., 1991, ApJ, 376, 380
[34] Dopita, M.A.& Ryder, S.D., 1994, ApJ, 430, 163
[35] Eggen, O.J., Lynden-Bell, D. & Sandage, A.R., 1962, ApJ, 136, 748
[36] Elbaz, D., Cesarsky, C. J., Fadda, D., Aussel, H. & al., 1999, A&A, 351, 37
[37] Ellison, S.L., Songaila, A., Schaye, J. & Pettini, M., 2000, AJ, 120, 1175
[38] Erb, D. K., Shapley, A.E., Pettini, M., Steidel, C.C., Reddy, N.A.& Adelberger, K.L., 2006, ApJ, 644, 813
[39] François, P., Matteucci, F. Cayrel, R., Spite, M., Spite, F. & Chiappini, C., 2004, A&A, 421, 613
[40] Garnett, D.R.& Shields, G.A., 1987, ApJ, 317, 82
[] Garnett, D.R., Skillman, E.D., Dufour, R.J.& Shields, G.A., 1997, ApJ, 481, 174
[41] Gibson, B.K. & Matteucci, F., 1997, ApJ, 475, 47
[42] Granato, G.L., Silva, L.,Monaco, P., Panuzzo, P., Salucci, P., De Zotti, G.& Danese, L., 2001, MNRAS, 324, 757
[43] Greggio, L. & Renzini, A., 1983, A&A, 118, 217
[44] Grevesse, N., & Sauval, A.J., 1998, Space Science Reviews, Vol. 85, p.161
[45] Goswami, A. & Prantzos, N., 2000, A&A, 359, 191
[46] Gunn, J. E. & Gott, J. R. III, 1972, ApJ, 176, 1
[47] Holweger, H., 2001, Joint SOHO/ACE workshop "Solar and Galactic Composition". Edited by Robert F. Wimmer-Schweingruber. Publisher: American Institute of Physics Conference proceedings Vol. 598, p.23
[48] Hachisu, I., Kato, M. & Nomoto, K., 1996, ApJ, 470, L97
[49] Hachisu, I., Kato, M. & Nomoto, K., 1999, ApJ, 522, 487
[50] Hamman, F. & Ferland, G., 1993, ApJ, 418, 11
[51] Henry, R.B.C., Edmunds, M.G.& Koeppen, J., 2000, ApJ, 541, 660
[52] Himmes, A., & Biermann, P., A&A, 1988, 86, 11
[69] Iben, I.Jr. & Tutukov, A.V., 1984, ApJS, 54, 335
[54] Ishimaru, Y., & Arimoto, N., 1997, PASJ, 49, 1
[55] Izotov, Y. I., Stasinska, G., Meynet, G., Guseva, N. G. & Thuan, T. X., 2006, A&A, 448, 955
[56] Jimenez, R., Padoan, P., Matteucci, F. & Heavens, A.F., 1998, MNRAS 299, 123
[57] Jorgensen, I., 1999, MNRAS, 306, 607
[58] Josey, S. A. & Arimoto, N., 1992, A&A, 255, 105
[59] Kauffmann, G., Charlot, S. & White, S. D. M., 1996, MNRAS 283, L117
[60] Kauffmann, G., White, S.D.M. & Guiderdoni, B., 1993, MNRAS, 264, 201
[61] Kennicutt, R.C. Jr., 1989, ApJ, 344, 685
[62] Kennicutt, R.C. Jr., 1998, ARAA, 36, 189
[63] Kobayashi, C. & Arimoto, N., 1999, ApJ, 527, 573
[64] Kodama, T., Yamada, T., Akiyama, M., Aoki, K., Doi, M., Furusawa, H.,Fuse, T., Imanishi, M. & al., 2004, ApJ, 492, 461

[65] Kobulnicky, H.A. & Skillman, E.D., 1996, ApJ, 471, 211
[66] Kroupa, P., Tout, C.A. & Gilmore, G., 1993, MNRAS, 262, 545
[67] Kuntschner, H., Lucey, J. R., Smith, R. J., Hudson, M. J. & Davies, R. L., 2001, MNRAS, 323, 625
[68] Hill, V., François, P., Spite, M., Primas, F., Spite, F., 2000, A&A, 364, L19
[69] Iben, I. Jr. & Tutukov, A., 1984, ApJ, 284, 719
[70] Iwamoto, K., Brachwitz, F., Nomoto, K., Kishimoto, N., Umeda, H., Hix, W. R. & Thielemann, F-K., 1999, ApJS, 125, 439 (I99)
[71] Lacey, C.G. & Fall, S. M., 1985, ApJ, 290, 154
[72] Lanfranchi, G. & Matteucci, F., 2003, MNRAS, 345, 71
[73] Lanfranchi, G. & Matteucci, F., 2004, MNRAS, 351, 1338
[74] Larson, R.B., 1972, Nature, 236, 21
[75] Larson, R.B., 1974, MNRAS 169, 229
[76] Larson, R.B., 1976, MNRAS 176, 31
[77] Larson, R.B., 1998, MNRAS, 301, 569
[78] Larson, R.B., & Dinerstein, H.L., 1975, PASP, 87, 911
[79] Lecavelier des Etangs, A., Desert, J.-M. & Kunth, D., 2003, A&A, 413, 131
[80] Lequeux, J., Kunth, D., Mas-Hesse, J. M. & Sargent, W. L. W., 1995, A&A 301, 18
[81] Lequeux, J.,Peimbert, M., Rayo, J. F., Serrano, A. & Torres-Peimbert, S., 1979, A&A, 80, 155
[82] Loewenstein, M., & Mushotzky, F., 1996, ApJ, 466, 695
[83] Maeder, A., 1992, A&A, 264, 105
[84] Maiolino, R., Cox, P., Caselli, P., Beelen, A., Bertoldi, F., Carilli, C. L., Kaufman, M. J., Menten, K. M.& al., 2005, A&A, 440, L51
[85] Maiolino, R., Nagao, T., Marconi, A., Schneider, R., Pedani, M., Pipino, A, Matteucci, F. & al., 2006, Mem. S.A.It. Vol. 77, 643
[86] Mannucci, F., Della Valle, M., Panagia, N., Cappellaro, E., Cresci, G., Maiolino, R., Petrosian, A. & Turatto, M., 2005, A & A, 433, 807
[87] Mannucci, F., Della Valle, M.& Panagia, N., 2006, MNRAS, 370, 773
[88] Marconi, G., Matteucci, F. & Tosi, M., 1994, MNRAS, 270, 35
[89] Martin, C.L., 1996, ApJ, 465, 680
[90] Martin, C.L., 1998, ApJ, 506, 222
[91] Martin, C.L., 1999, ApJ, 513, 156
[92] Martinelli, A., Matteucci, F. & Colafrancesco, S., 2000, A&A 354, 387
[93] Matteucci, F., 2001, *The Chemical Evolution of the Galaxy*, ASSL, Kluwer Academic Publisher
[94] Matteucci, F.,1994, A&A, 288, 57
[95] Matteucci, F. & Chiosi, C., 1983, A&A 123, 121
[96] Matteucci, F. & François, P., 1989, MNRAS 239, 885
[97] Matteucci, F.& Gibson, B.K., 1995, A&A 304, 11
[98] Matteucci, F., Raiteri, C. M., Busso, M., Gallino, R. & Gratton, R., 1993, A&A, 272, 421
[99] Matteucci, F. & Greggio, L., 1986, A&A ,154, 279
[100] Matteucci, F., Molaro, P. & Vladilo, G., 1997, A&A 321, 45
[101] Matteucci, F. & Padovani, P., 1993, ApJ, 419, 485
[102] Matteucci, F. & Recchi, S., 2001, ApJ 5,58, 351
[103] Matteucci, F.& Tornambé, A., 1987, A&A, 185, 51
[104] Matteucci, F., & Vettolani, G., 1988, A&A, 202, 21

[105] McWilliam, A. & Rich, R. M., 1994, ApJS, 91, 749
[106] Menanteau, F., Jimenez, R.& Matteucci, F., 2001, ApJ, 562, L23
[107] Meynet, G. & Maeder, A., 2002, A&A, 390, 561
[108] Moretti, A., Portinari, L. & Chiosi, C., 2003, A&A, 408, 431
[109] Nomoto, K., Hashimoto, M., Tsujimoto, T., Thielemann, F.-K. & al., 1997, Nucl. Phys. A, 616, 79
[110] Oey, M. S., 2000, ApJ, 542, L25
[111] Padovani, P. & Matteucci, F., 1993, ApJ, 416, 26
[112] Papaderos, P., Fricke, K. J., Thuan, T. X. & Loose, H.-H., 1994, A&A 291, L13
[113] Pardi, M.C., Ferrini, F. & Matteucci, F., 1994, ApJ, 444, 207
[114] Peletier, R. 1989, PhD Thesis, University of Groningen, The Netherlands
[115] Pilyugin, I.S., 1993, A&A 277, 42
[116] Pipino, A., Matteucci, F., Borgani, S. & Biviano, A., 2002, NewAstr., 7, 227
[117] Pipino, A., Matteucci, F., 2004, MNRAS, 347, 968
[118] Pipino, A., Matteucci, F., 2006, MNRAS, 365, 1114
[119] Portinari, L. & Chiosi, C., 2000, A&A, 355, 929
[120] Prantzos, N., 2003, A&A, 404, 211
[121] Prantzos, N. & Boissier, S., 2000, MNRAS 313, 338
[122] Recchi, S., Matteucci, F. & D'Ercole, A., 2001, MNRAS 322, 800
[123] Recchi, S., Matteucci, F., D'Ercole, A. & Tosi, M., 2004, A&A, 426, 37
[124] Renzini, A., 2004, in *Clusters of Galaxies: Probes of Cosmological Structure and Galaxy Evolution*, eds. J.S. Mulchay, A. Dressler & Oemler, A. (Cambridge University Press), p.260
[125] Renzini, A. & Ciotti, L., 1993, ApJ, 416, L49
[126] Renzini, A., Ciotti, L., D'Ercole, A. & Pellegrini, S., 1993, ApJ 416, L49
[127] Rothenflug, R. & Arnaud, M., 1985, A&A, 144, 431
[128] Salpeter, E.E., 1955, ApJ, 121, 161
[129] Sandage, A., 1986, A&A, 161, 89
[130] Scalo, J.M., 1986, Fund. Cosmic Phys. 11, 1
[131] Scalo, J.M., 1998, *The Stellar Initial Mass Function*, A.S.P. Conf. Ser., Vol. 142 p.201
[132] Schechter, P., 1976, ApJ, 203, 297
[133] Schmidt, M., 1959, ApJ, 129, 243
[134] Schmidt, M., 1963, ApJ, 137, 758
[135] Schneider, R., Salvaterra, R., Ferrara, A. & Ciardi, B., 2006, MNRAS, 369, 825
[136] Searle, L. & Zinn, R., 1978, ApJ, 225, 357
[137] Skillman, E.D, Terlevich, R. & Melnick, J., 1989, MNRAS, 240, 563
[138] Springel, V. & Hernquist, L., 2003, MNRAS, 339, 312
[139] Tamura, T., Kaastra, J.S., den Herder, J.W.A., Bleeeker, J.A.M. & Peterson, J.R., 2004, A&A, 420, 135
[140] Thielemann, F.K., Nomoto, K. & Hashimoto, M., 1996, ApJ, 460, 408
[141] Thomas, D., Greggio, L., Bender, R., 1999, MNRAS, 302, 537
[142] Thomas, D., Maraston, C., Bender, R. & Mensez de Oliveira, C., 2005, ApJ, 621, 673
[143] Thomas, D., Maraston, C.& Bender, R., 2002, in: R.E. Schielicke (ed.), Reviews in Modern Astronomy, Vol.15, p.219
[144] Thuan, T.X., Izotov, Y.I., Lipovetsky, V.A., 1995, ApJ, 445, 108
[145] Tinsley, B.M., 1980, Fund. Cosmic Phys., Vol. 5, 287

[146] Tinsley, B.M. & Larson, R.B., 1979, MNRAS, 186, 503
[147] Tornambé, A., 1989, MNRAS, 239, 771
[148] Tosi, M., 1988, A&A, 197, 33
[149] Tosi, M., Aloisi, A., & Annibali, F., 2006, IAU Symp. N.35, p.19
[150] Tozzi, P., Rosati, P., Ettori, S., Borgani, S., Mainieri, V.& Norman, C., 2003, ApJ, 593, 705
[151] Tremonti, C.A., Heckman, T. M., Kauffmann, G., Brinchmann, J., Charlot, S., White, S. D. M.; Seibert, M., Peng, E. W. & al., 2004, ApJ, 613, 898
[152] Tsujimoto, T., Shigeyama, T. & Yoshii, Y., 1999, ApJ 519,63
[153] van den Hoek, L.B. & Groenewegen, M.A.T., 1997, A&AS, 123, 305 (HG97)
[154] Vladilo, G., 2002, A&A, 391, 407
[155] Vigroux, L., 1977, A&A, 56, 473
[156] Weiss, A. Peletier, R. F. & Matteucci, F., 1995, A&A, 296, 73
[157] Whelan, J. & Iben, I. Jr., 1973, ApJ, 186, 1007
[158] White, S.D.M., & Rees, M.J., 1978, MNRAS 183, 341
[159] Wills, B.J., Netzer, H. & Wills, D., 1985, ApJ, 288, 94
[160] Worthey, G., 1994, ApJS, 95, 107
[161] Worthey, G. Faber, S. M. & Gonzalez, J. J., 1992, ApJ, 398, 69
[162] Worthey, G, Trager, S.C., Faber, S. M., 1995, ASP Conf. Ser., 86, 203
[163] Woosley, S.E. & Weaver, T.A., 1995, ApJS, 101, 181 (WW95)
[164] Wyse, R.F.G. & Gilmore, G., 1992, AJ, 104, 144
[165] Wyse, R. F. G.& Silk, J., 1989, ApJ, 339, 700